Review on automated 2D material design

2D Materials

TOPICAL REVIEW

Review on automated 2D material design

Abdalaziz Al-Maeeni[1], Mikhail Lazarev[1], Nikita Kazeev[3], Kostya S Novoselov[3] and Andrey Ustyuzhanin[2,3,*]

[1] HSE University, Myasnitskaya Ulitsa, 20, Moscow 101000, Russia
[2] Constructor University, Campus Ring 1, Bremen 28759, Germany
[3] Institute for Functional Intelligent Materials, National University of Singapore, 4 Science Drive 2, Singapore 117544, Singapore
[*] Author to whom any correspondence should be addressed.

E-mail: andrey.ustyuzhanin@constructor.org

Keywords: deep learning, material science, 2D materials, materials generation, inverse design

OPEN ACCESS

RECEIVED
10 January 2024

REVISED
10 April 2024

ACCEPTED FOR PUBLICATION
2 May 2024

PUBLISHED
6 June 2024

Abstract

Deep learning (DL) methodologies have led to significant advancements in various domains, facilitating intricate data analysis and enhancing predictive accuracy and data generation quality through complex algorithms. In materials science, the extensive computational demands associated with high-throughput screening techniques such as density functional theory, coupled with limitations in laboratory production, present substantial challenges for material research. DL techniques are poised to alleviate these challenges by reducing the computational costs of simulating material properties and by generating novel materials with desired attributes. This comprehensive review document explores the current state of DL applications in materials design, with a particular emphasis on two-dimensional materials. The article encompasses an in-depth exploration of data-driven approaches in both forward and inverse design within the realm of materials science.

1. Introduction

Most scientific laws are formulated to solve forward problems; they predict the properties of a system given its initial conditions. In contrast, inverse problems involve inferring the underlying causes, factors, or structures responsible for a set of observations. These problems arise in two key contexts. In the first case, inverse problems are solved to deduce physical laws, relations, or a humble parameter value from the experimental data. In the second, we put scientific knowledge to practical use and create an object with the desired properties. Attempts to solve inverse problems have been undertaken in a wide range of fields: engineering, material science, non-destructive testing (NDT), geophysics, radiation therapy, computational fluid dynamics, medical imaging, geology, astronomy, and economics; we list some of the most interesting examples in the appendix A.

Over the last decade, remarkable progress in material science has been achieved, significantly pushing forward many applications, from electronics to energy, composite materials to membranes. Consequently, the development of materials with predetermined properties has become critical for numerous critical technologies.

The inverse problem in material science arises in many different areas, from mechanics to the atomic structure of materials, from spectroscopy data analysis to material design [1–5]. This article focuses on a specific facet: determining the composition and structure of a 2D crystal based on its macroscopic physical properties, such as strength, elasticity, conductivity, *etc*.

Material discovery is a complex process with a general workflow that can be broken down into several parts, as depicted in figure 1. Firstly, new material candidates are generated, and their suitability for potential applications is simulated. Next, the material with the highest likelihood of success is synthesized. Lastly, the material is incorporated into a device and its desired properties are investigated. The time required to design a material is thus dependent on three factors: (i) the number and duration of simulations, (ii) the duration of synthesis of proposed candidates, and (iii) the time needed for measurements

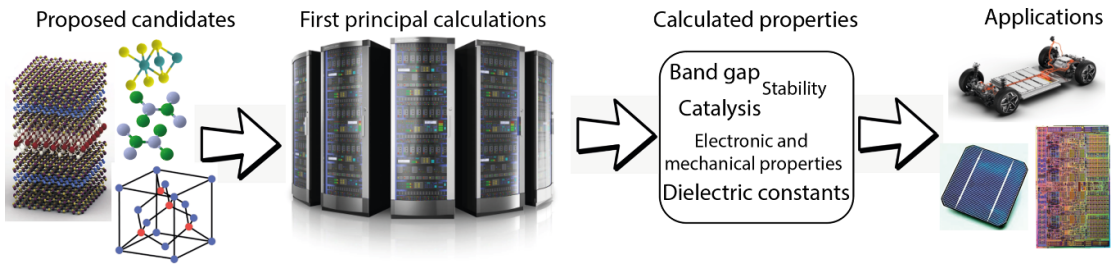

Figure 1. The classical material design workflow. Candidate materials are intuitively perceived and their properties are computed in silico and verified experimentally.

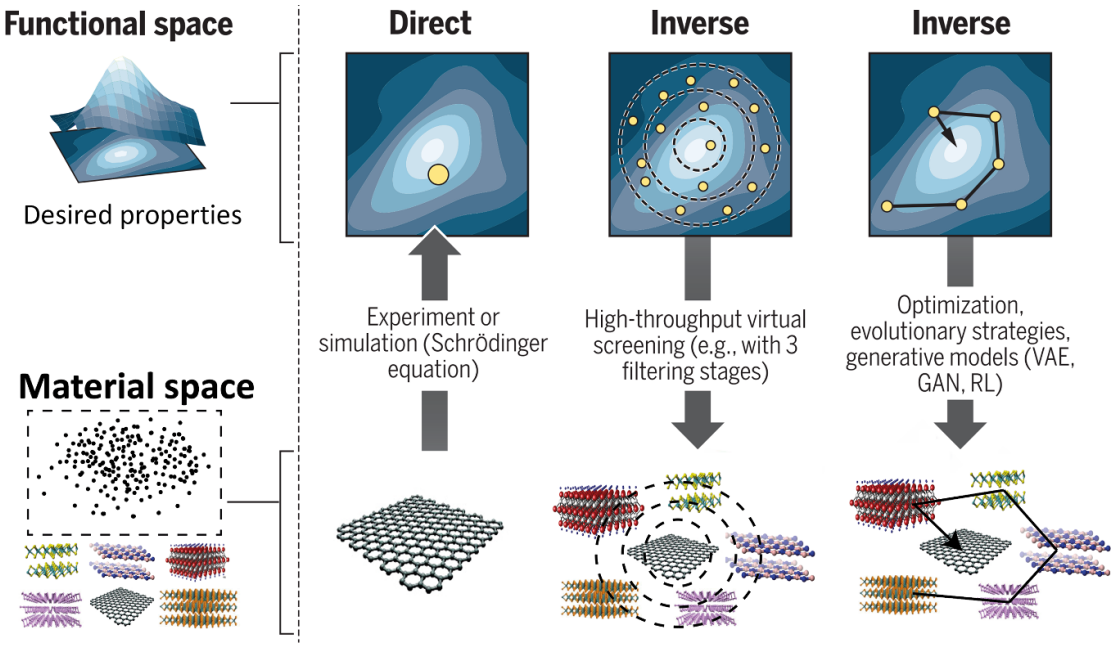

Figure 2. Schematic illustration of material and functional space and different approaches toward materials design. From [7]. Reprinted with permission from AAAS.

and the selection of the best candidates. The usual material's discovery or optimization time is measured in years [6] and requires significant human and computational resources. The inverse design approach aims to accelerate the process of discovery of new materials by efficiently and accurately finding candidates in silico.

A schematic overview of material design problems and their possible solutions is presented in figure 2, where we link the material space and the material functional space.

This paper is structured as follows. In section 2.1, we discuss the simulation of materials based on physical principles; in section 2.2 we review structure representations suited for machine learning (ML); in section 2.3—property prediction based on ML. Section 3 is dedicated to the inverse problem; in section 3.1 we cover high-throughput virtual screening technique; in section 3.2—evolutionary design methods; in section 3.3—generative ML methods; in section 3.4—the recent applications of the reinforcement learning (RL) approach. Section 4 concludes the paper with a discussion of the methods' applicability and general outlook.

2. Material simulation

2.1. Ab-initio methods

In the 20th century, the formulation of quantum mechanics solved the principal problem of theoretical atomic systems description. However, the many-body Schrodinger equation is too complex to be directly solved for most real-world systems. Hence, a number of approximate methods was developed. One of the most widely used approaches for materials is density functional theory (DFT) [8]. It allows for relatively efficient calculation of the electron ground state and its properties, such as the energy and the band structure, etc. DFT has been used to generate huge material databases [9] and to train ML algorithms

Table 1. Generic material datasets.

Dataset	Size	URL
QM7, QM7b, QM8, QM7bml, QM9, QM7-X	>100 k	http://quantum-machine.org/
Alchemy	200 K	https://alchemy.tencent.com/
ANI-1	20 M	https://github.com/isayev/ANI1_dataset
ANI-1x	5 M	https://github.com/aiqm/ANI1x_datasets
AGZ7	140 k	https://github.com/binghuang2018/agz7/tree/master
tmQM	80 k	https://github.com/bbskjelstad/tmqm
OQMD	>1 M	https://oqmd.org/
The Open Catalyst	>1 M	https://opencatalystproject.org/
AFlow	3.5 M	www.aflowlib.org/
Materials Project	>600 k	www.materialsproject.org
Materials Cloud	>10 M	www.materialscloud.org/home

Table 2. Crystal structures datasets with 2D materials.

Dataset	Size	URL
Aflow	3.5 M	www.aflowlib.org/
JARVIS-DFT	77 k	https://jarvis.nist.gov/
C2DB	4 k	www.cmr.fysik.dtu.dk/c2db/c2db.html
aNANt	23 k	www.anant.mrc.iisc.ac.in
Materials Cloud	>10 M	www.materialscloud.org/home
2DMatPedia	6 k	www.2dmatpedia.org/
Materials Project	>600 k	www.materialsproject.org
ICSD	300 k	www.psds.ac.uk/icsd
COD	500 k	www.crystallography.net/cod/
CSD	1 M	www.ccdc.cam.ac.uk/
OQMD	300 k	https://oqmd.org/
QPOD	2 k	https://cmr.fysik.dtu.dk/qpod/qpod.html
2DMD	>15 k	https://rolos.com/open/2d-materials-point-defects/
2D Materials	6 k	https://cmr.fysik.dtu.dk/c2db/c2db.html

[10]. The computation time of DFT is proportional to the cube of the number of atoms in the structure [11, 12], with the practical system size ceiling of around 1000 atoms. Taking advantage of the interaction locality allows the use of DFT for larger systems with computational time linearly dependent on the number of atoms [13], but provides little advantage for small systems. The accuracy of DFT in describing nanoscale material properties has led to its widespread adoption in various scientific software packages, a complete list of which can be found in Wikipedia[4].

Several DFT-derived databases cataloging an array of structures, from molecules to crystals, have been made available for diverse research objectives. We enumerate the principal online datasets in table 1. Some of these databases contain a wide variety of structure types, including 2D materials. In table 2, we have collected databases containing 2D materials. It is worth mentioning that a much more extensive list of datasets suitable for training ML algorithms to predict material properties is available[5]. Despite the breadth of these resources, the exhaustive landscape of materials and their properties remains incompletely mapped. This prompts ongoing efforts by research collectives to compile specialized datasets tailored to specific investigational needs [14].

The exploration of large atomic systems with more than a thousand atoms is predominantly facilitated through molecular dynamics (MD) simulations. In MD, atoms are treated as classical particles that interact with each other; classical MD deals with only forces, energies, and stress—without simulating electrons in any way. It is a very powerful set of methods for predicting mechanical properties. In a simple case, MD uses heuristic interatomic interaction potentials (EIP); providing a computationally efficient means to simulate systems comprising up to 10^6 atoms. However widely used set of interatomic simulations like Tersoff [15], AIREBO [16], ReaxFF [17], and optimized Tersoff [18] can fail in seemingly straightforward simulations, such as those involving graphene [19]. Each atomic system needs carefully selected inter-atomic potential and its parameters. *Ab initio* MD (AIMD) overcomes this issue by mixing DFT and MD, but these methods are limited by computational cost since they rely on DFT.

Since the interatomic interaction potentials are by their nature heuristic approximations, ML has been systematically and successfully used to train

[4] https://en.wikipedia.org/wiki/List_of_quantum_chemistry_and_solid-state_physics_software.

[5] https://github.com/JuDFTteam/best-of-atomistic-machine-learning.

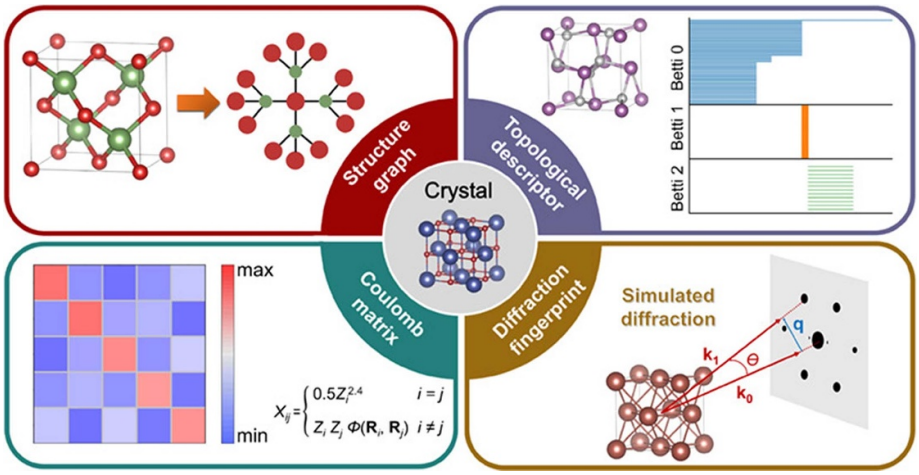

Figure 3. One crystal can be represented in various ways using different representations. These representations include: a graph containing atom and bond weights, Coulomb matrix, diffraction fingerprint, using topological descriptors and etc. [43] John Wiley & Sons. © 2021 Wiley Periodicals LLC.

ML interatomic potentials (MLIP) on the DFT data, starting with [20]. Modern methods [21–23] provide accuracy comparable to DFT with EIP computational speed. Now MLIPs can be used in MD simulations using either generic packages like LAMMPS [24], as well as within specialized packages like TorchMD [25] and DeepMD [26]. Nowadays MLIPs are greatly used in material simulations, acceleration of materials design [27–29], and predicting material properties [30]. There are few types of MLIPs: neural network potentials (NNPs) [20, 23, 31], Gaussian approximation potentials (GAPs) based on Gaussian process regression [32], moment tensor potentials [33, 34], spectral neighbor analysis potentials [35], deep tensor neural networks [36], Gaussian moment NNPs [37] and most recently neuroevolution-potentials [38]. In comparison to EP, MLIPs, as other ML methods, rely heavily on the quality and diversity of training data, trained using DFT-based datasets in combination with AIMD data, including high-temperature regimes, to take into account diverse atomic environments. Temperature effects represent a huge niche where MLIPs are found to be more accurate than traditional DFT and EP [21]. MLIPs have shown particular promise in the research of two-dimensional (2D) materials. For instance, they have been applied to study 2D lattices of biphenylene [39], quasi-hexagonal-phase C_{60} fullerene ($qHPC_{60}$) [40], BC_2N [41], MoS_2 [42].

2.2. Atomic structure representation

The core problem of building a model of a given structure is the mathematical representation of an atomic system. Suppose we follow Born–Oppenheimer approximation and presume that the electrons are in the ground state. In that case, the atomic system is fully described as a set of atoms, their positions, and momenta. Using the raw coordinate values as algorithm input is counterproductive as this does not respect the rotation, translation, and permutation equivariance and quickly leads to a problem of intractable computational complexity. A good representation must respect those symmetries. There are two observations that are usually useful when constructing such representations. Firstly, most atomic-scale properties are continuous and smooth functions of the atomic coordinates. Representations that preserve this smoothness are preferred. Secondly, representation usually loses a certain amount of information. Discarded information might limit the accuracy of the model.

Early interatomic interaction potentials used just the pairwise distances [44] to compute pairwise forces. While conceptually simple and computationally efficient, this approach can not describe complex interactions. More advanced descriptors were primarily based on fingerprints driven by chemical intuition [45–48], and molecular and crystal graphs [49–52]. Modern empirical interatomic potentials [53–55] are typically expressed as an additive combination of local terms and long-range pairwise contributions. Hence, additive, atom-centered representations have become popular in molecular ML.

Other possible material representations include structure fingerprints [56], inspired by the Fourier transform Diffraction fingerprints [57], which are widely used as crystal descriptors. Coulomb matrices [58] each element is calculated based on the Coulombic interactions between atoms. The diagonal elements reflect the properties of individual atoms, while off-diagonal elements represent interactions between different atoms. As it is schematically depicted in figure 3. And other methods like: bags of bonds [59], Indicators from quantum chemical calculations [60], empirical valence bond method [61], SPRINT method [62], Overlap matrix eigenvalue fingerprints [62, 63].

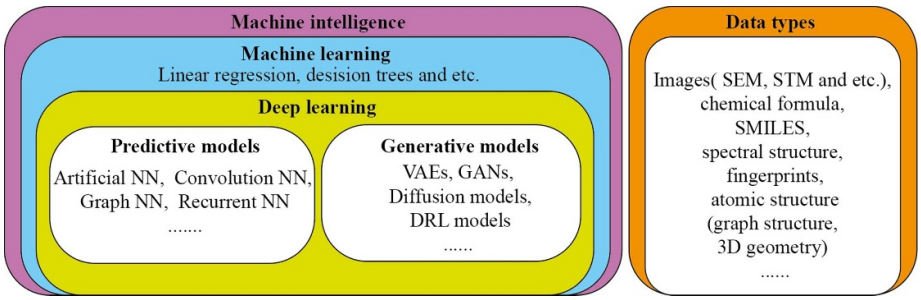

Figure 4. Different sub-fields of machine intelligence.

Topological descriptors [43], particularly those based on persistent homology, are advanced tools used in materials science to encode compounds' structural information. They work by representing chemical structures as a series of interconnected points (like a 3D point cloud), capturing the structure's local and global details.

Voxel-based representations [64] naturally preserve translation-invariant features and provide a rich input to computer-vision inspired neural networks, but until recently [65] suffered from the lack of a way to encode the rotation symmetry.

Graph representation of an atomic system [66] respects all the symmetries and also provides for interaction locality. It is used in most state-of-the-art ML methods. We will discuss it in more detail in the next section 2.3.

In small organic molecules, most information about the structure can be recovered from just a graph of atoms and bonds between them. This allows grammar-based representation, exemplified by the Simplified Molecular Input Line Entry System (SMILES) [67], to be commonly used to represent them. However, it is limited to stereochemistry types, has no standard for handling aromaticity, and no way to generate canonical representation [68]. The recent development of SELFIES [69] as next-generation molecule text representation has the potential to overcome some of these limitations. However, the SMILES or SELFIES methods cannot be used to describe crystal structure yet because crystal representation must satisfy translational, rotational, and permutational invariances. In a recent article, the first string-based method for representing crystal structures SLICES was presented [70].

The methods mentioned here are by no means an exhaustive list. Musil *et al* [71] provided an excellent review of the different methods used for the structure representation of molecules and crystals. The choice of representation ultimately depends on the available data. While numerous databases are readily accessible online [9], 2D material datasets remain limited. However, the field is rapidly evolving with the availability of new datasets [72–74], and further research is required to explore the potential of different material representations fully.

2.3. Machine learning

Machine intelligence or Artificial intelligence is a rapidly growing field encompassing ML and deep learning (DL). ML is a subfield of artificial intelligence concerned with developing algorithms and statistical models that enable computer systems to learn from data and make predictions or decisions based on that data. In contrast, DL is a specific subset of ML that uses artificial neural networks to perform tasks that require a high degree of abstraction, such as image and speech recognition, natural language processing, and the applications of other scientific domains [75]. The relationship between the fields is depicted in figure 4.

While both ML and DL involve training algorithms on data to make predictions or decisions, they differ in their approach to learning and the types of problems they are best suited for. ML typically relies on hand-crafted features usually designed by domain experts, reflecting their priors and inductive biases to capture the relevant information in the data. In contrast, DL models learn to extract relevant features directly from the data using multiple layers of interconnected nodes that can learn increasingly abstract representations of the data. Reflecting the biases and the symmetries into those layers is usually more complicated, as it requires the introduction of invariances and equivariance into the definition of the layers.

The ability of DL models to automate feature selection is a significant advantage over traditional ML methods. This advantage has been demonstrated in numerous applications, including images [76], speech recognition [77], natural language processing [78], game playing [79], protein folding [80]. For example, in material science, DL models have been used to predict or classify material properties without involving hand-crafted features. Ma *et al* [81] used a combination of DL and *ab initio* calculations to discover novel 2D ferroelectric materials. Wilhelm *et al* [82] employed various DL methods to predict the

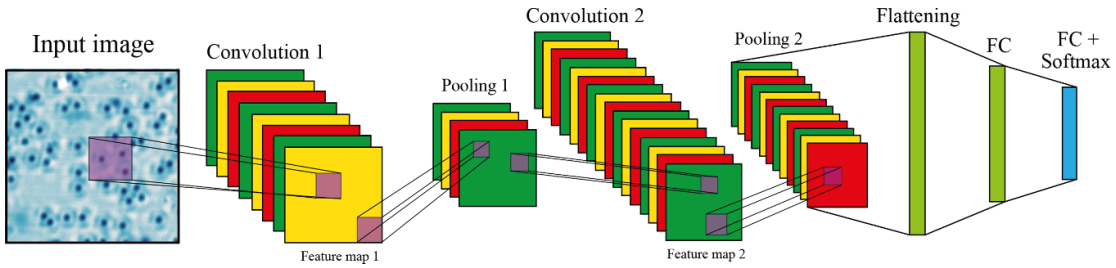

Figure 5. Convolution neural network. The 2D material image. Reproduced from [88]. CC BY 4.0.

physical properties of Van der Waals heterostructures from their constituent monolayer properties.

ML can be broadly classified into three categories: supervised learning, unsupervised learning, and RL. In supervised learning, a model is trained on labeled datasets of input-output pairs to learn the underlying relationship between the input and output variables. On the other hand, unsupervised learning involves training a model on an unlabeled dataset to discover patterns and structure in the data, relying on metric distances and differences between samples. RL is a type of learning in which an agent learns to interact with an environment to maximize a reward signal.

The development of machine intelligence has led to numerous breakthroughs in fields such as computer vision, natural language processing, and robotics. With the availability of large amounts of data and the development of powerful computing hardware, the potential of machine intelligence to revolutionize various industries and sectors is enormous. Goodfellow *et al* [75] provide a comprehensive overview of ML and DL, including their classifications, applications, and challenges.

In recent years, ML algorithms have been extensively used for predicting or classifying material properties. For instance, decision trees, support vector machines [83, 84], and other ML methods have been applied to 2D materials [85, 86]. Wilhelm *et al* [82] employed different ML methods, including AdaBoost, Elastic Net, Gradient Boosted Trees, Kernel Ridge Regression, and Support Vector Regression, to predict the physical properties of Van der Waals heterostructures from their constituent monolayer properties.

Convolution neural networks (CNNs) [87] are highly effective in DL, specifically for spatial data. Convolutional layers use kernels to scan the input, which is typically discretized on a grid, and the same filter is used multiple times with different positions in the input. Such parameter sharing makes training CNNs more efficient. Translation invariance is also an essential feature of convolution. It is particularly important for image processing because features such as edges and shapes can be present anywhere in the case of images; thus, convolution helps capture these features regardless of their location.

Another useful feature is local connectivity. Convolutional layers use kernels with varying spatial extent. The schematic illustration of simple CNN is presented in figure 5. This local connectivity allows the network to capture local patterns in the structure or the image, such as edges, corners, texture in the case of images, or atom types and other physics-based descriptors e.g. structure density, volume per atom, maximum packing fraction, structural complexity [89], XRD powder pattern [90], orbital field matrix [91], and JarvisCFID [92]. Combining multiple convolutional layers with different filters can capture increasingly complex patterns, allowing the network to learn hierarchical representations of the input. Usually, convolutional layers are followed by pooling or reduction layers, designed to reduce the spatial resolution of the input while retaining the most important information. This helps to make the network more robust to small movements after translation translations and deformations in the input and also reduces the number of parameters that need to be learned.

The main issue with utilizing the regular CNN (where the domain of the operation is defined as a grid) for materials science is that the locations of atoms and molecules are usually not restricted to a grid, and their precise locations carry important information that will be lost if discretized to a grid. Based on that, the authors of SchNet [93] develop a continuous filter convolution where the input is not required to be embedded on a grid. SchNet is designed to learn a representation for predicting different physical attributes, mainly energies and atomic forces. The model is invariant with respect to translation and permutations of atom indexing, with a smooth energy prediction w.r.t. perturbation to atom positions and energy conservation of the predicted force fields. The energy and force predictions are rotationally invariant and equivariant, respectively. At the time, SchNet demonstrated state-of-the-art results on the QM9 [94, 95] dataset and accurate results for MD17 [96] and ISO17 [93].

2.3.1. Graph neural networks

Graph neural networks (GNNs) [97, 98] are an important class of ML algorithms that operate on

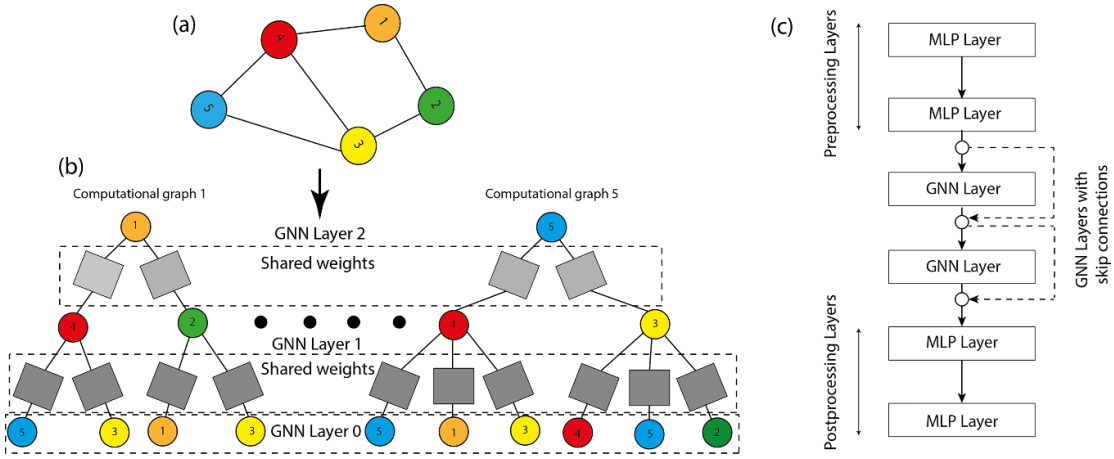

Figure 6. Convolutional GNN (a) example of graph structure (b) for each node computational graph is constructed, where each layer contains aggregation functions with shared waits across that layer (c) upscaled vision of CGNN.

graph-structured data. Mathematically, a graph consists of two sets: nodes V (alternatively called vertices) and edges E. An edge connects two vertices, hence $E \subset V^2$. A graph can have additional data associated with its elements, typically called node and edge features.

Such general and straightforward definitions make graphs a suitable mathematical model for a wide variety of data. For example, images can be presented as a graph structure with a regular grid-like structure, with individual pixels representing nodes and RGB channel values at each pixel serving as node features. CNNs have shown a great ability to extract features from image-like data. Thus, it would be natural to generalize this idea to graphs of any kind. A rectangular convolutional filter expects a fixed number of pixels as its input. The weights also depend on the relative position of the pixels. A graph, however, does not have a natural ordering of the neighbors and can have an arbitrary number of them. Therefore, in a graph convolution, every neighboring node participates with the same weight.

Consider a graph example in figure 6(a) that can represent a small molecule. Figure 6(b) depicts how the two-layer classic convolutional GNN looks like for that graph. The first layer (layer 0) consists of just node feature vectors, which serve as an input to GNN layers. For each node, we define a computational graph that differs from node to node and depends on node surroundings, but the depth is the same for all of them. Node 1 6(b) aggregates and processes information by a nonlinear function, which may be by itself a small NN. The information aggregation from node neighbors and neighbors of its neighbors, such aggregation is called two-hop aggregation or two layers of GNN block. Usually, there is no need to have a large number of GNN layers unless you are working with graphs of high diameter. To make GNN more expressive, the post and pre-processing layers and residual connections can be added as schematically shown in 6(c). The second way to improve GNNs is to modify the GNN blocks by themselves.

GNNs have been successful in many applications [99]. Recently, GNNs have found application in materials science, showing promise in tasks such as crystal structure prediction and property prediction.

In the context of crystal structure prediction, GNNs can be used to model the interactions between atoms in a crystal lattice and predict the resulting arrangement of atoms. This approach has proven highly effective, with some studies reporting accuracy comparable to the traditional *ab initio* computational methods, such as DFT calculations [66, 100].

One of the key advantages of GNNs for materials science applications is their ability to handle large and complex graph structures, which is often the case for crystal structures. Additionally, GNNs can be trained on large datasets, allowing them to capture complex patterns in the data that are not easily modeled using traditional methods.

As a result, GNNs have been actively researched in the field of materials science in recent years, with a growing body of literature demonstrating their effectiveness for a variety of tasks. In one of the earliest works that used GNNs for crystal properties prediction, [66], the authors use Graph Convolutional Neural Network with the representation of the elementary cell of the crystal in the form of a graph, taking into account periodicity (see figure 7). The information about atoms is stored in the graph nodes, while graph edges represent interatomic distances.

The next significant advancement in this field involved the application of methods based on a more advanced variant of GNN, known as the message-passing neural network. MatErials Graph Network (MEGNet) [101] is designed to address the limitations of existing ML models. It incorporates global state attributes (see figure 8) and allows

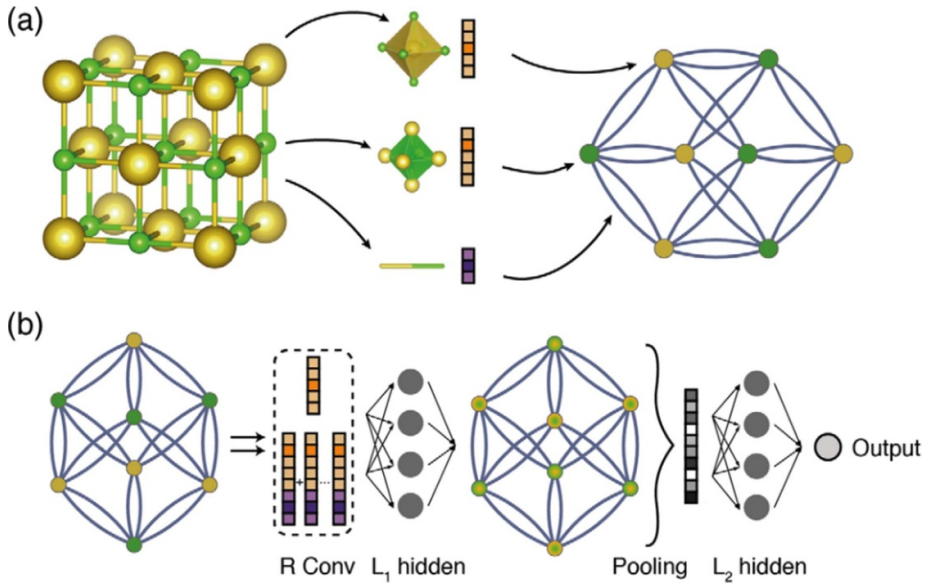

Figure 7. CGNN. Illustration of the crystal graph convolutional neural networks. (a) Construction of the crystal graph. Crystals are converted to graphs with nodes representing atoms in the unit cell and edges representing atom connections. Nodes and edges are characterized by vectors corresponding to the atoms and bonds in the crystal, respectively. (b) Structure of the convolutional neural network on top of the crystal graph. R convolutional layers and L_1 hidden layers are built on top of each node, resulting in a new graph with each node representing the local environment of each atom. After pooling, a vector representing the entire crystal is connected to L_2 hidden layers, followed by the output layer to provide the prediction. Reprinted with permission from [66], Copyright (2018) by the American Physical Society.

for composability. The MEGNet models outperform prior ML models in predicting properties such as internal energy, enthalpy, Gibbs free energy, formation energies, band gaps, and elastic moduli. MEGNet also presents two strategies to address data limitations in materials science and chemistry. These strategies include a physically-intuitive approach to unify multiple free energy MEGNet models into a single model and using transfer learning from a larger data set to improve property models with smaller amounts of data.

However, constructing the edges of the structure graph based on the atoms pairwise distances fails to account for the directional information between atoms. To address this issue, Gasteiger *et al* [102] developed a GNN model that embeds directional information in the form of message transformations based on the angle between two atoms. The transformed messages are then propagated using the message-passing mechanism. Notably, the embeddings of the directional messages are rotational equivariant. DimeNet [102] utilizes the spherical Bessel function and spherical harmonics to construct an orthogonal representation of directional messages. This approach achieves better performance with fewer parameters (75% reduction) compared to the standard Gaussian radial basis representation used by SchNet.

DimeNet++ [103] is an improved version of DimeNet that addresses the issue of combinatorial representation explosion by reducing the number of embeddings in the directional message passing block. In the original DimeNet, every message between interacting pairs is embedded separately, resulting in a combinatorial explosion of embeddings. The situation becomes worse in the interaction block, where every triplet is embedded to represent the bond angles. This makes operations in the directional message passing block 15x more expensive than elsewhere in the model. To address this issue, DimeNet++ replaces the bilinear layer used in the original directional message passing block with a simple Hadamard product and compensates for the loss in expressiveness by adding multilayer perceptrons (MLPs) for the basis representations. This results in the same accuracy as the original DimeNet, at a fraction of the computational cost. DimeNet++ also leverages the fact that certain parts of the model use a higher number of embeddings by reducing the embedding size in these parts via down- and up-projection layers. This both accelerates the model and removes information bottlenecks. In addition to these improvements, the authors found that using four layers performs similarly to the original six for some energy prediction tasks. They also observed that larger batch sizes significantly slowed down convergence, and mixed precision caused the model precision to break down completely. However, the relative error of DimeNet is below float16's machine precision, which, indeed, can be expected.

GATGNN [104] is another variant of GNNs based on the attention mechanism. It introduces a model based on GNNs composed of multiple graph-attention layers and a global attention layer

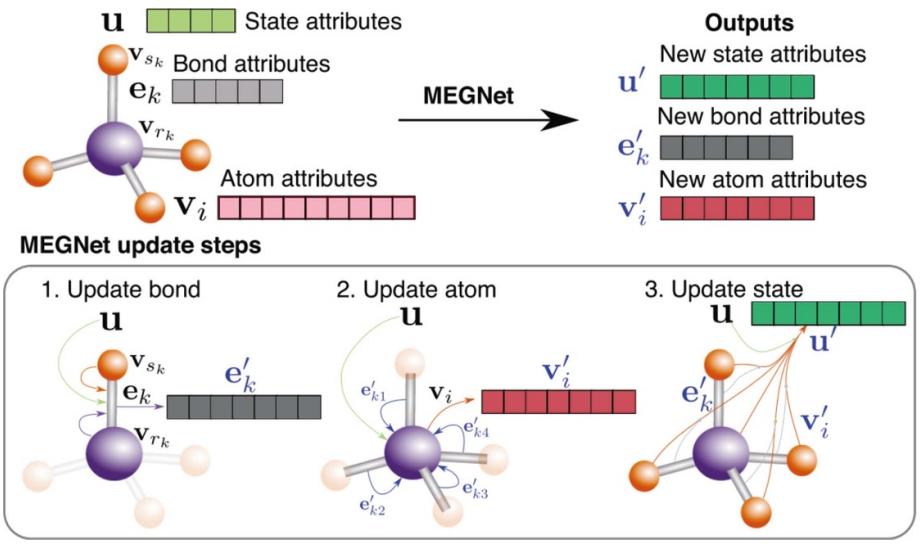

Figure 8. An overview of a MEGNet module. The initial graph is represented by the set of atomic attributes $V = v_i$, bond attributes $E = \{(e_k, r_k, s_k)\}$, and global state attributes u. In the first update step, the bond attributes are updated. Information flows from atoms that form the bond, the state attributes, and the previous bond attribute to the new bond attributes. Similarly, the second and third steps update the atomic and global state attributes, respectively, by information flow among all three attributes. The final result is a new graph representation. Reprinted with permission from [101]. Copyright (2019) American Chemical Society.

to predict inorganic material properties. The model learns the complex bonds shared among the atoms within each atom's local neighborhood, and the global attention layer provides the weight coefficients of each atom, improving the model's performance. This approach allows the model to capture the different contributions of the atoms in the crystal to the global material property. The paper highlights the limitations of existing structural descriptors and the characteristics of desired structural descriptors. It discusses the use of GNNs in material property prediction and introduces the attention mechanism to learn the contribution of different context vector components to the merged context vector.

GemNet [105] is an improved architecture that is based on DimeNet++. The architecture of GemNet incorporates three different forms of interaction: geometric message passing, one-hop geometric message passing, and pure atom self-interaction based on atom embeddings. Ablation studies have shown that all three interaction forms benefit the model's performance. While two-hop message passing introduces significant computational overhead, it is mitigated by a down-projection layer and by the ablated GemNet-T model. Interestingly, the GemNet-T model performs remarkably well on the MD17 dataset, but not on COLL. The author suggests that one-hop message passing is expressive enough for certain practical use cases. In contrast, two-hop message passing provides an advantage for more challenging tasks that involve fitting multiple molecules at once. In typical ML models, the variance of activations is stabilized using normalization methods, which have been shown to have various positive effects on training. However, these methods can have undesirable side effects in the context of molecular regression. To address these issues, GemNet stabilizes its variance by introducing constant scaling factors, as suggested by Brock *et al* [106]. Skip connections, non-linearities, message aggregation, and Hadamard/bilinear layers primarily impact the activation variance. Simple empirical scaling factors are sufficient to keep the activation variance roughly constant. Other measures, such as adaptive gradient clipping, scaled weight standardization, or weighting the residual block with zero at initialization, turn out to be not very beneficial for the accuracy of the model. In summary, GNNs have gained widespread popularity in the field of material property prediction. They naturally provide desirable inductive bias by respecting symmetries and interaction locality and demonstrate state-of-the-art performance. Being DL methods with a large number of parameters, they benefit greatly from the increased amounts of data.

3. Material design

3.1. High-throughput screening

High-throughput screening (HTS) can be viewed as the most straightforward computational material design technique. It consists of an expert-provided algorithm for generating candidate materials and a computational module that predicts the target properties of a material. It can work either ab-initio or using ML. The success of HTS depends on the quality of the initial screening scope, which experts in the field should carefully define. To reduce the cost of HTS, computational funnels may be used, in which cheaper or easier-to-compute properties are used as initial filters, with more sophisticated methods or

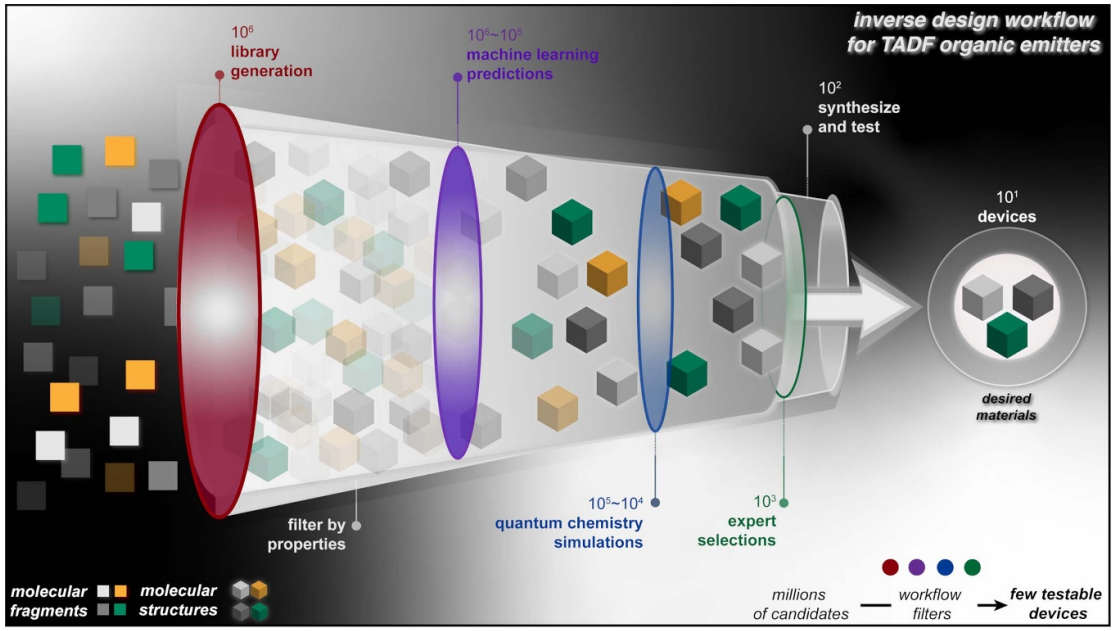

Figure 9. HTS for screening thermally activated delayed fluorescence organic emitters, starting from selecting fragments to the device integration. Reproduced from [107]. CC BY 4.0.

properties used to narrow down the pool of candidates for final selection. An example HTS pipeline is presented in figure 9.

HTS has been successful in identifying a variety of materials [108–110]. Zhang *et al* [111] review the use of high-throughput computational screening and data mining to discover 2D materials.

In another study [112], the authors present several examples of the use of computational screening to identify promising 2D materials for various applications. They use DFT calculations to screen a dataset of over 150 Na-based layered materials, identifying potential sodium-based battery electrodes with desirable properties such as high average voltage, high sodium ion mobility, and low volume change during the intercalation/de-intercalation of Na ions. In addition, the authors show the use of HTS to identify 2D photocatalysts with positive phonon dispersions, indicating that they may be experimentally exfoliated.

First-principles calculations combined with HTS are used to identify quantum spin Hall insulators, materials with a specific type of topological order that could be used in spintronic devices [113–118].

ML methods have played an important role in identifying layered, exfoliatable materials. Exfoliation techniques, such as mechanical cleavage, surfactant-assisted ultrasonication, and ion intercalation, remain a popular way to prepare various 2D materials. These techniques have played a significant role in the exfoliation of 2D materials from their corresponding layered bulk materials, such as graphene, TMDs, MXenes, and phosphorene [113, 119–123]. Therefore, finding materials that can be exfoliated is an important task.

Mounet *et al* in [113] performed high-throughput calculations using van der Waals DFT to predict easy exfoliating 2D materials. More than 100 000 unique crystal structures were extracted from public databases for selection using a specially designed protocol. As a result, more than 5000 structures were filtered and classified as layered structures. In the second stage, selected structures were validated with DFT computations. The result of the study is 1036 candidate materials for easy exfoliation.

HTS search performance is limited by the candidate evaluation speed, and ML offers an obvious way. The paper by Noh *et al* [124] is a typical example of this work. They combine DFT, ML, and HTS. The authors use pre-trained ML to do the initial screening, followed by DFT, for more precise estimation. The authors built on the crystal convolutional neural network (CGCNN) [125] model, which we discuss in section 2.3.1. They modified it in two ways. First, they use the hyperbolic tangent instead of softplus as the activation function, which regularizes the latent vector within the range of $(-1, 1)$. This causes crystal feature vectors with similar properties to be clustered in the latent space. Secondly, they use Monte Carlo dropout [126] to quantify the uncertainty of the predictions. It generates multiple slightly different copies of the model by randomly dropping some connections between neurons. The diversity among the predictions of the model copies is treated as an uncertainty estimate.

In a recent article [127], a combined approach using various methods for generating new crystalline structures was also proposed, along with a vast number of DFT calculations to determine their properties.

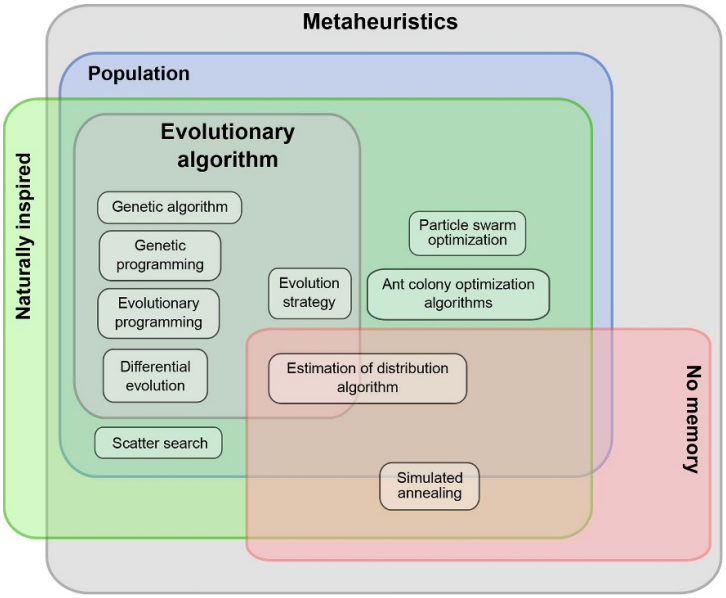

Figure 10. Classification of metaheuristics algorithms. Reproduced from [131]. CC BY 3.0.

The article suggests and implements scaling the initial dataset for material research through active learning. For this purpose, a pipeline was proposed for generating crystalline lattices of various structures and compositions, unlike those presented in the initial dataset. The generated candidate structures are filtered by a GNN and further calculated using DFT. This iterative method of enriching the database was proposed to yield hundreds of thousands of stable structures. Some were selected as targets for synthesis in an automated laboratory and were obtained experimentally [128].

Overall, high-throughput computational screening accelerated by ML and data mining offers a powerful tool for discovering novel 2D materials, and the research community expects that these methods will continue to play a significant role in the development of materials science. By using materials databases and computational methods based on advancements in ML, researchers can efficiently gather, access, store, and analyze materials data, facilitating the design of materials with specific properties and applications. These methods have already led to the discovery of several promising 2D materials with potential applications in areas such as energy storage and electronics, and they have the potential to identify other functional 2D materials, such as 2D superconductors, photocatalysts, and photoelectronic materials.

3.2. Evolutionary and global optimization

Evolutionary methods are a class of metaheuristic algorithms that are used for solving complex optimization problems that involve a large number of variables and constraints. Biological evolution processes, swarm behavior, and physical laws inspire these algorithms. Evolutionary methods are broadly classified into two categories: single-solution based and population-based metaheuristic algorithms; see figure 10 for details. Single-solution based metaheuristics use a single candidate solution and improve it using local search, but they may get stuck in local optima. Population-based metaheuristics use multiple candidate solutions to maintain diversity in the population and avoid getting stuck in local optima [129]. Those methods avoid local minima at the cost of computing multiple evolution processes at once.

Genetic algorithm (GA) is one of the most widely used evolutionary methods miming the Darwin theory of survival of the fittest in nature [130]. The basic elements of GA include encoding the problem at hand in some representation, usually a bit-vector, fitness selection function, and biological-inspired operators such as selection, mutation, and crossover.

The principle of GAs is to start with a population of potential solutions representing a set of possible solutions to the optimization problem. Each solution is evaluated based on a fitness function that measures how well it solves the problem. The solutions with higher fitness are more likely to be selected for reproduction.

Reproduction involves selecting two solutions from the population and creating a new solution (offspring) by combining parts of the two parents. This process is called crossover. The offspring may also undergo random mutations, where a small portion of the solution is changed randomly. The idea behind mutation is to introduce new solutions into the population that may not have been explored before, analogous to local search.

The refreshed population, comprising parents and offspring, undergoes the same selection cycle, crossover, and mutation. This iterative process is

repeated for several generations, typically until a stopping criterion is met, such as a maximum number of generations or a minimum acceptable fitness value.

Over successive generations, the population gradually converges toward superior solutions, driven by the selection process that favors solutions with higher fitness scores. The genetic operators of crossover and mutation introduce diversity into the population, which helps avoid getting stuck in local optima.

The success of GAs is due to their ability to explore a large search space efficiently and find good solutions even in the presence of noise, uncertainty, and the lack of gradient information.

Evolutionary algorithms have a rich history of being used for inverse design [132, 133]. In the rest of the section, we review notable cases of their application for designing 2D systems.

In [134] Andreas Håkansson and Jose Sanchez-Dehes present a method for the inverse design of photonic crystals (PhCs) [135, 136] using a GA. PhCs are materials with unique properties that can be used to design optical devices with sub-wavelength cavities and low loss. These materials have potential applications in various fields, including telecommunications, sensors, and energy harvesting [137–139]. While traditional design methods rely on physical intuition and insight into PhCs nature. In contrast, the inverse design enables the optimization of functional devices based on predefined constraints. This approach has been used to design a variety of PhC components, including spot-size converters [140], photonic bandgap materials [141], cavities for QED experiments [142], low loss PhC waveguide (WG) bends [143].

In particular, the work [144] considers the design of a de-multiplex WG coupler (DEMUXWGC). The purpose of the device is to separate and couple two wavelengths from a single dielectric WG to two separate PhC-WGs. The design variables for the DEMUXWGC are the coupling efficiency and crosstalk attenuation for each channel and wavelength. To estimate these parameters, the authors calculate the amplitudes of the electric field in the center of the PhC WGs. Since the PhC-WG is designed to support a single mode, the total intensity flux of the coupled mode can be scaled proportionally with the maximal amplitude of the mode profile.

Kildishev *et al* [145] use evolutionary methods to design a three-layer near-field lens, a lens designed to operate on a scale much smaller than the wavelength of light. The authors use three optimization methods: simulated annealing (SA), which is based on the physical analogy of cooling crystal structures; a GA; and particle swarm optimization (PSO). SA had the best result.

The authors also note that the practical fabrication of optimal devices requires taking additional considerations into account, such as geometrical limitations, material properties, and the impact of the fabrication process on material properties. These constraints can affect the performance of the materials and must be considered in the design process. Overall, the authors demonstrate the successful use of optimization techniques for the design of metamaterials for nanoscale optical sensing and imaging.

Hassan and Tallman in [146] present a study on the use of global search algorithms to solve the inverse problem of computing strains from conductivity changes in self-sensing materials [147–153]. The authors explore the use of three commonly used metaheuristic global search algorithms, namely SA based on [154, 155], PSO based on [156–158] and GA based on the work of [159, 160] to solve the ill-posed, multi-modal inverse problem. The study is motivated by the current limitations in determining the underlying mechanical state of a piezoresistive sensor from electrical measurements. Based on the experimental loading setup, the authors formulated a boundary value problem (BVP) of a plate consisting of an unknown displacement boundary condition. The BVP was integrated with the finite element method to solve for the optimum displacement boundary condition. The SA, PSO, and GA algorithms were used to find the solution to the BVP. The authors chose parameter values for the algorithms based on the observation that the plate did not fail during the experiment and the expected applied displacement to be lower than the failure displacement. The study results indicate that the three global search algorithms were able to find solutions to the inverse problem of computing strains from conductivity changes. The authors draw a quantitative comparison between the three algorithms regarding the quality of the inversely computed displacements and strains, the variability and accuracy of the displacement solutions, and the computational efficiency regarding the fitness function and runtime.

Zhao *et al* [161] employ an evolutionary algorithm USPEX combined with *ab initio* simulations [162–164] to search for structural phases of 2D boron allotropes with the goal of discovering new superconducting phases. The authors use the monolayer, bilayer, and thin multilayer 2D boron structures to study superconductivity and perform searches based on the spacing between layers of multi-walled boron nanotubes. The results of the study reveal five energetically stable structures with high symmetry. The authors find that superconductivity is ubiquitous in these newly found boron structures, with T_c values higher than the liquid-helium temperature. The authors attribute the high T_c values to the presence of multiple vibration modes in the electron–phonon coupling mechanism.

Study of Na_xCl_y systems at various conditions by USPEX algorithm [165] predicted two exotic stable compounds, Na_3Cl and Na_2Cl were found at normal conditions as 2D phases on a graphene substrate

[166]. There are many other USPEX predictions applied to 2D materials [167, 168].

Bahmann and Kortu in [169] developed an evolution strategy-based algorithm for crystal structure prediction called EVO. The algorithm uses crystal structures as individuals and Gibbs free energy as the fitness function that must be minimized. The authors also employed variable-cell structure relaxation [170], which provides an efficient local optimization and makes the structures and energies comparable for a global search.

The author's implementation of EVO has been successfully applied to find crystal structures of elements in the 3rd main group, encompassing various space groups and utilizing different multiples of the number of atoms in the conventional cell. The authors also found 2D structures, such as a boron sheet, with structural features not previously considered in the literature.

Two-dimensional magnetic materials have attracted significant attention due to their potential applications in spintronics and data storage [171–177]. Stimulated by these exciting experimental reports, 56 new magnetically ordered monolayer structures were predicted from high-throughput computation to be exfoliated from known magnetic bulk materials [113]. To search for stable 2D magnetic structures, the authors further developed a new computational scheme based on the *ab initio* evolutionary algorithm USPEX [162–164] combined with the spin-polarized DFT. The initial structures are randomly produced with assigned layer group symmetry and user-defined thickness. They are assumed to have either ferromagnetic, anti-ferromagnetic or nonmagnetic (NM) orders. User inputs determine the ratio of different structures (NM, FM-LS, FM-HS, AFM-LS, AFM-HS, FM-LSHS, and AFM-LSHS). The authors evaluated the reliability and accuracy of their new method by investigating the 2D CrI_3 system. Through this search, they uncovered many new metastable magnetic structures that had not been previously identified in high-throughput computational screenings. Additionally, these structures did not have any known parent bulk materials in the database, indicating that the search was not biased and offered a more comprehensive sampling of the configuration space. The most stable magnetic structure contained 19 atoms per unit cell and was identified as the `19-P6/mmm` borophene as a stable striped-AFM semiconductor.

Chen *et al* in [178] have proposed a GA for designing high-performing optical sensors, focusing on the use of transition metal dichalcogenide (TMDC) Bloch surface wave (BSW) technology. This technology offers advantages such as an all-dielectric structure, sharper resonance peaks, and a wider wavelength range. However, previous studies have demonstrated that the sensitivity of BSW sensors is typically lower than that of surface plasmon resonance sensors when using the standard Kretschmann prism coupling method. To enhance the sensitivity, the researchers proposed a multi-variable, multi-objective optimization method utilizing an improved GA. By optimizing such factors as film thickness, periods of one-dimensional PhC, the thickness of the defect layer, and the number of layers of TMDC materials, they were able to increase the sensitivity of the sensor significantly. The highest sensitivity was reached using $MoSe_2$, WSe_2, MoS_2, or WS_2, resulting in an improvement of 24.3%, 24.8%, 22.7%, or 24.4% respectively. This optimized BSW sensor has potential applications in various fields, including food safety, environmental monitoring, and biological analysis.

Mishra *et al* in [179] propose an approach to training and quantifying quantum MD (QMD) simulations. The team introduced a multi-objective GA (MOGA)-based approach for the reactive MD (RMD) method. The method enables large-scale simulations of chemical events in complex materials involving multimillion atoms. The approach is used to study the high-temperature sulfidation of MoO_3 flakes with H_2S precursors during the chemical vapor deposition synthesis of MoS_2 monolayers. The goal was to train ReaxFF [180] parameters against QMD simulations by estimating the number of H–S, Mo–O, and Mo–S bonds as a function of time. The results showed that the MOGA-based approach for RMD was able to reproduce the time evolution of key reaction events in the QMD simulations.

Patra *et al* in [181] presents a new strategy of utilizing neural networks combined with GAs to design soft materials without pre-existing databases efficiently. This strategy involves the selection of new candidates for the GA based on an objective function that quantifies their properties in relation to target values. The authors note that this approach enables the GA to learn from its history, accelerating the process compared to an evolutionary process alone.

GAs have also been combined with MD to study defects. For example, later, Patra *et al* in the paper [182], investigate the extended structure of point defects and their dynamical evolution in transition-metal dichalcogenides. A fundamental understanding of the atomic-scale structure and dynamics of defects in these low-dimensional systems and their role in phase transitions is critical for advances in nanotechnology.

This study combines ML methods with MD simulations to study how point defects in a 2D monolayer of MoS_2 are organized into extended structures. The authors use high-resolution transmission electron microscopy experiments to validate their findings and show how defects evolve from random point defects to extended line defects, which play a role in driving phase transitions from a semiconducting 2 H phase to a metallic 1 T phase. Simulations and experiments suggest that the alignment of the extended line defects influences the size and shape of the 1 T regions. By introducing them into a MoS_2 layer, the

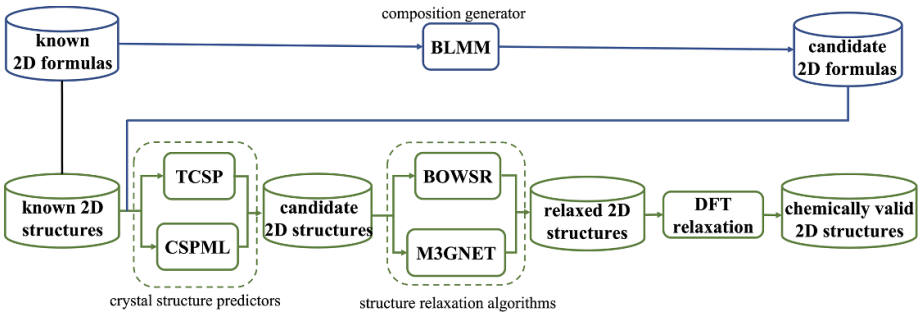

Figure 11. The process for generating 2D materials. It describes the architecture of a material transformer generator (MTG) pipeline. Reproduced from [183]. CC BY 4.0.

relative proportions of the metallic and semiconducting phases can be systematically controlled.

3.3. Machine intelligence

ML works by fitting a heuristic, 'intuitive' model for the system under study, on the high level, it is the same for both forward and inverse problems. Designing a new material, is, however, a much more difficult problem than predicting properties. Instead of summarizing the information about a given structure and predicting a number, the algorithm must traverse the intractable space of all possible arrangements of elements and find one that is stable and has different properties.

3.3.1. Generative modeling

As we discussed previously, raw atomic structures do not match well with the ML mathematical and computational apparatus. Hence, generative methods map the structures into a more suitable representation, learn the probability distribution inside this space, and then map from it to the structures. A common aspect of all the methods developed so far is that this second mapping does not fully define the structures, but just provides an initial guess which is then refined using the forward models.

An illustrative approach of this kind is present in figure 11 Dong *et al* in [183] propose a material transformer generator, a pipeline for 2D material discovery that integrates a transformer-based 2D material composition generator, two template-based crystal structure predictors, and a GNN potential-based structure relaxation algorithm.

Firstly, the material composition is mapped into a sequence and sorted by electronegativities of elements. The distribution over those sequences is learned using Transformer [184] in the step called blank language models for materials. Notice the information loss.

Secondly, the initial guesses for the structures are produced using two crystal structure prediction algorithms: template-based crystal structure prediction (TCSP) [185] and ML-based crystal structure prediction (CSPML) [186]. TCSP is based on oxidation state patterns, while CSPML uses a ML model to select templates based on structural similarity. For a new 2D formula, both TCSP and CSPML would first select all template structures with the prototype ABC3, but the sorting process differs between the two. TCSP focuses on element distance and calculates the element mover distance score and element oxidation states. On the other hand, CSPML selects candidates solely based on the topological features of the atomic coordinates and does not use any information about the elemental composition.

Thirdly, two ML potential-based relaxation algorithms are used to optimize the structures. These algorithms are BOWSR [187], which uses Bayesian optimization with symmetry relaxation and M3GNet [31], which utilizes materials GNNs with 3-body interactions as an energy estimation model.

Finally, the formation energy and e-above-hull energy of structures are calculated using DFT.

A set of known 2D formulas and their structures were collected from open datasets, including C2DB, MC2D, 2DMatPedia, and V2DB. The pipeline was trained using materials from various databases (328 719 formula samples and 12 214 structures).

Variational autoencoder (VAE) is a generative model that consists of two main parts: encoder and decoder [188] similar to autoencoders (AEs) (see figure 12 VAE). The VAE core idea is to learn the latent probability space representation of objects presented in a dataset. Sampling vectors from learned latent space and decoding them should give us a new object similar to what is presented in the training dataset.

Noh *et al* in [189] introduced the first VAE generative model for inverse crystal design. This work proposed a framework to learn continuous material representation in a latent space. The algorithm consists of three steps. Firstly, it represents the material as a 3D image, by diving the space into voxels, and atoms as balls. The second step is training an AE to transform the images into a latent vector. Finally, a

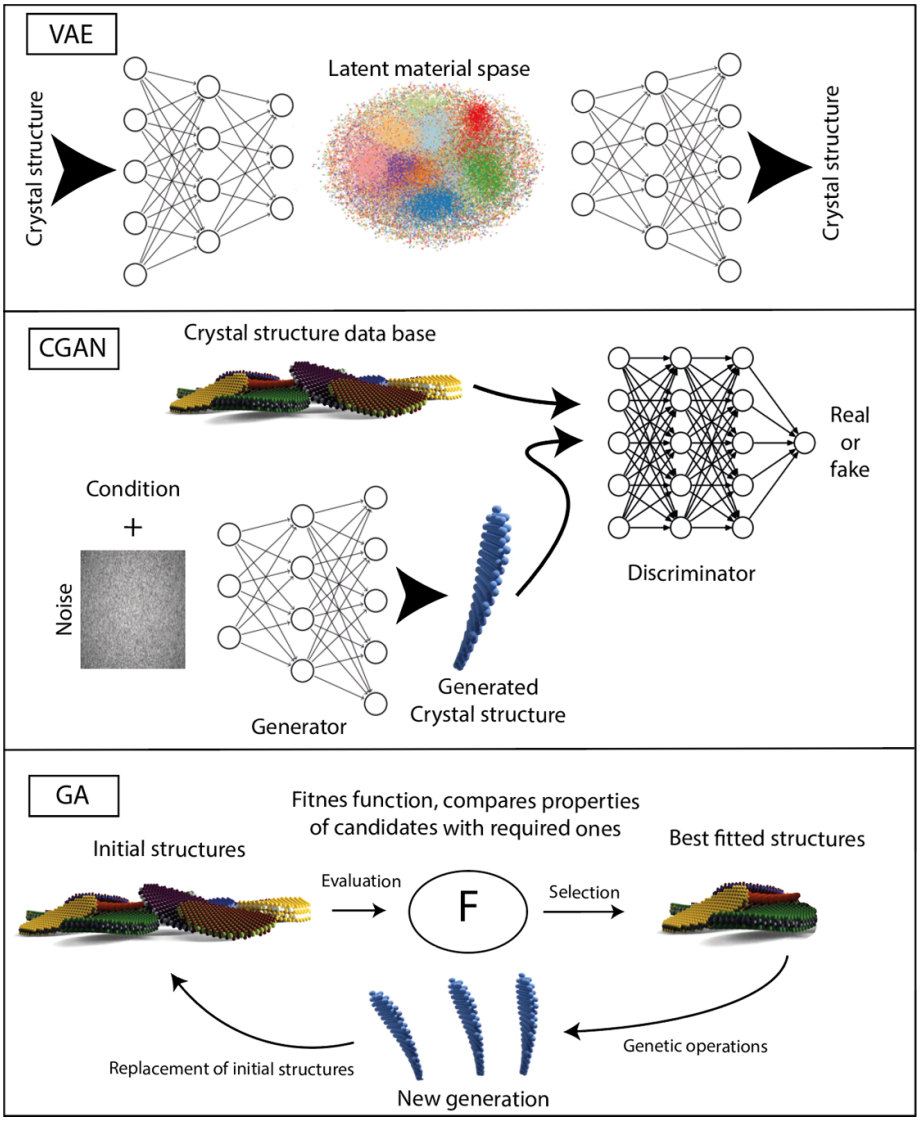

Figure 12. Schematic illustration of VAE, conditional GAN, and genetic algorithms.

VAE is trained to generate new materials in this latent space. The model was trained and tested on a custom VO dataset comprising 10 981 V_xO_y compounds. The authors reported newly generated metastable VO structures and supported their findings with DFT simulations.

The Crystal Diffusion Variational AutoEncoder (CDVAE) [190] uses a GNN to map the materials into a latent vector space. An MLP is used to predict the lattice parameters and chemical composition from a latent vector. Finally, a random unit cell with those parameters is generated and is relaxed using a denoising model. CDVAE has been shown to outperform past methods in tasks such as reconstructing input structures, generating diverse and realistic materials, and creating materials with specific optimized properties.

The latest model that employs diffusion was presented by the Microsoft research team [191]. MatterGen is a diffusion model that generates stable, diverse inorganic materials across the periodic table and can be fine-tuned to the generation of materials with a wide properties range. The noise introduction process is designed to independently disrupt the types of atoms, coordinates, and lattice to achieve a physically motivated picture of the randomized material. The equivariant scoring network was pretrained for denoising. The authors claim that, compared to the previous solutions, their model produces materials that are more than twice likely to be new and stable, and also that the model predicts the energy of the material 15 times closer to the local energy minimum.

A VAE was also trained in [192]. A conditional type of VAE is used to learn a continuous representation of the materials in a latent space. This research explores the space of 2D materials from the point of view of photocatalysts: these substances can be used for photocatalytic water splitting, a technique to produce hydrogen. This is a task of significant

importance since hydrogen as transport fuel promises to alleviate the effects of global warming. The authors use a database containing the properties of 2D materials computed via high-throughput DFT calculations [193]. Based on this data, a generative model learns the representations of 2D materials to generate novel ones sampling from continuous representations. The pipeline to learn the representations of the 2D materials consisted of 'cell' and 'basis' AEs and a segmentation network like in the iMatGen framework. The analysis of the predictions of the 'cell' and 'basis' encodings was then used to train a conditional VAE, whose latent space was sampled to generate new 2D materials. Subsequently, the novel materials were constrained and narrowed down to qualify as potential catalysts. As a result of passing the ∼150 materials through a classification network, 19 materials with a probability of >0.99 belong to the stable class. Moreover, it was observed that all 19 shortlisted appeared to be halides since they were the dominant type in the training dataset.

Generative adversarial networks (GANs) represent a class of generative models initially designed to tackle image generation problems as VAEs. GANs are composed of two neural networks, generator and discriminator [194] (see figure 12 GAN). As an input to the generator, it used a Gaussian noise vector, which the generated output discriminator takes as an input to judge if it is a real object or a generated one. During the training, both NNs compete with each other. Thus, generative NN can be trained to generate objects that are hardly distinguishable from those presented in the dataset.

One of the classic examples of generative model usage was presented in [195]. The generative model was applied to metasurface properties prediction and metasurface pattern generation. The core of the generative algorithm is a conditional deep convolutional generative adversarial neural network (CGAN).

Kim *et al* [196] is one of the first examples where conditional GANs were used in tandem with a critic neural network to generate crystals on the base of Mg–Mn–O ternary materials using an image-like representation. They also use a variant of GAN that utilised Wasserstein distance [197] between generated material target value distribution and target distribution for additional training stability.

In a recent work by Long *et al* [198], GANs with constraints similar to algorithm architecture as in [196] were applied to crystal structure generation. Here, encoding of the lattice constants and atomic positions is done by training the AE to learn latent material representation space, which can be represented as an image. Overall, 50 000 structure image representations were generated. However, only 9160 was reasonable because most of the generated structures contained atoms that occupies the same position. 8310 structures among them are distinct. Thus, it was shown that CCDCGAN is capable of reproducing known structures and pushing boundaries by predicting new materials.

In research by Song *et al* [199] GAN with random forest (RF) classifier was proposed as a part of a generative inverse design algorithm to discover new 2D materials. To generate chemically valid compositions at the first stage, GAN learns to generate chemically valid formulas from known datasets. RF classifier trained on a mixed dataset of 2D materials and non-2D used to assign a probability for generated material from the GAN of being 2D material. Here, the probability was used as a ranking criterion, and 1485 hypothetical materials were generated with a probability of more than 0.95. DFT simulations were performed to determine exfoliation energy. As a result, 31 materials were found to have exfoliation energies of less than 200 meV, thus potentially easy to exfoliate. However, the proposed algorithm has its weaknesses; as the authors mentioned, the crystal structure prediction is a weak place here since it uses template-based structure prediction. To generate novel material with a unique structure, a more powerful structure prediction algorithm is needed.

Text-based generation. With the recent explosion of interest in language models (LM), two preprints [200, 201] suggest generating material structures as token sequences using Transformer [184]. They try two modes: with character-level tokenization, the model generates structures as text files, character-by-character. With atom+coordinate-level tokenization, the model discretizes the atomic coordinates, and uses the resulting bins as coordinate tokens, and generates them together with atom type tokens. The authors claim performance comparable to physically-motivated state-of-the-art models, for generating both crystals and organic molecules. The LM do not respect any kind invariance (permutation, translation, rotation), which makes these ongoing developments even more fascinating. Was the problem that simple all along?

3.4. Reinforcement learning

RL [203] is one of the ML methods during which the model (so-called agent) learns to achieve a goal. Unlike supervised learning, which relies on a static dataset for training, RL is characterized by an agent interacting with a dynamic environment, learning from the consequences of its actions through a trial-and-error strategy. RL methods are widely used in robotics and automated systems. Together with modern achievements in robotics, they allow for automatic atomically precise material construction, and opens up a way to inverse material design on the surface.

Chen *et al* [202] propose to use an RL-assisted experimental method to build atom-by-atom Ag patterns on a Ag(111) surface. The method is further

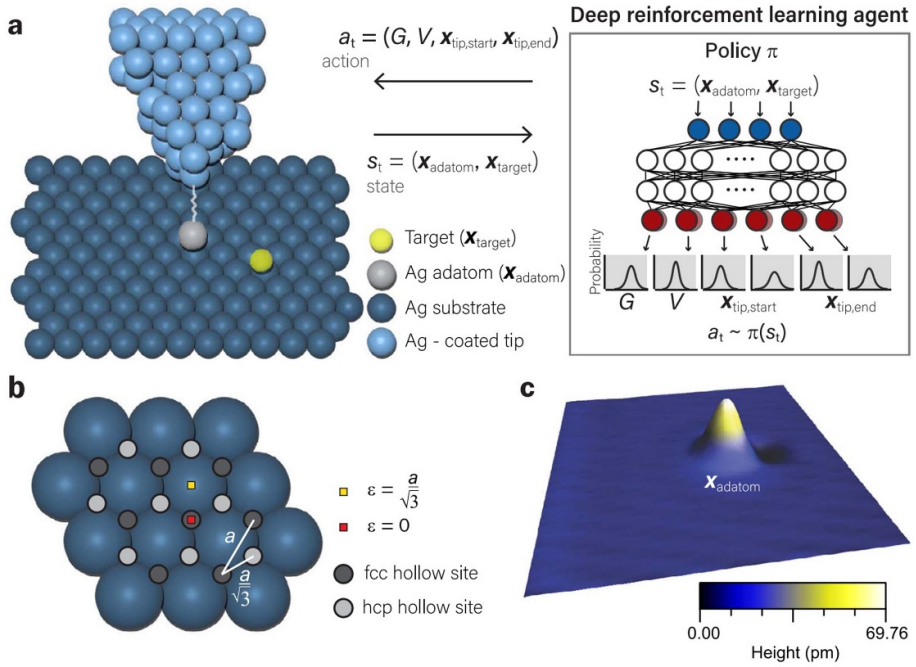

Figure 13. (a) The RL agent learns to manipulate atoms precisely and efficiently through interacting with the STM environment. STM is operated via actions (commands) a_t consisting of conductance G, bias V, and the two-dimensional tip position at the start and end of the manipulation $\boldsymbol{x}_{\text{tip, start}}$, $\boldsymbol{x}_{\text{tip,end}}$, which are used to move the STM tip to try to move the adatom to the target position. The agent samples the actions from a distribution (the so-called policy) $\pi(\text{st})$, where it is the state vector consisting of the current and target adatom positions. The policy π is modeled as a multivariate Gaussian distribution with mean and covariance given by a neural network. (b) The atom manipulation goal is to bring the adatoms close to the target position as possible. (c) STM image of an Ag adatom on Ag substrate. Reproduced from [202]. CC BY 4.0.

described in figure 13. The interaction of the tip and the atoms is difficult to describe theoretically with sufficiently accurate prediction, and RL allows us to automatically learn the manipulation of specific adatoms with a specific STM machine experimentally.

Banik *et al* [204] use an RL method to search for optimal defect patterns in MoS_2. The study proposes to use Monte Carlo Tree Search to explore the defect configuration space and identify potentially stable configurations and evolution paths towards them.

3.5. Simulation-based inference

Simulation-based or likelihood-free inference methods are used in various scientific domains to infer the underlying parameters of complex systems. This complexity may stem from a generative or simulating process. However, inferring these parameters poses a significant challenge due to the intractability of the likelihood function (a mapping from observed data to parameters) and the necessity to align simulation model parameters with prior knowledge derived from domain expertise and empirical data. Bayesian inference tackles this challenge by furnishing a framework for inverting simulations.

The typical intractability of the likelihood of observed data given parameters, a vital component for statistical inference, renders traditional statistical methods inapplicable. In simulation-based inference, the statistical model is defined by the simulator itself, with parameters in the model that describe the underlying mechanism and influence the transition probabilities. Moreover, latent variables are integral to the simulation, and the structure of the latent space may vary among simulators.

Various approaches can be used to utilize simulation-based inference for materials design. These approaches share common components: the simulator (e.g DFT algorithms), proposed distribution, and inference method. The simulator's parameters are drawn from the proposal distribution, and the simulator's output is either used directly or as input for a surrogate model, subsequently employed for inference.

There are two broad categories of inference techniques: those that utilize the simulator directly during inference (e.g. approximate Bayesian computation [205–207]) and those that construct a surrogate model for inference. The former compares the simulator output directly to the data, while the latter trains a surrogate model using the simulator's output as training data for the estimation or ML stages [208–210]. The relationship between the latter category and generative models is explored in the works of Mohamed and Lakshminarayanan [211], Louppe *et al* [212].

In Bayesian inference, the ultimate goal is to obtain the posterior distribution of the parameters. Some methods provide samples of parameter points

from the posterior, while others yield a tractable function approximating the posterior. The decision on which quantities to infer can be made early or postponed, depending on the method used.

In the probabilistic programming paradigm [213], the simulator is written in a probabilistic programming language. Utilizing a probabilistic programming language allows for sampling from the posterior distribution of input parameters and latent variables given observed data. These techniques, based on Markov chain Monte Carlo or training a neural network for proposal distributions, differ from ABC in that the inference engine controls all steps in program execution and biases each draw of random latent variables to enhance the simulation's likelihood of matching observed data, thereby improving sample efficiency. These algorithms facilitate not only the inference of input parameters, but also the entire latent process leading to a specific observation.

Simulation-based inference can be utilized in materials design, offering insight into material properties and performance under various conditions, thereby informing the design process. For a more comprehensive analysis, Cranmer *et al* [214] provides an excellent review of simulation-based inference.

4. Discussion and outlook

In this article, we review the state of the art in ML for material design. The main data-driven methods and their applications for forward and inverse design in materials science were considered. ML methods in the scope of 2D materials have yet to show their full potential. The main limiting factor is the small amount of data available for training models and still huge material search space.

Due to the high computational cost of HTS methods (like DFT), only a fraction of the desired materials and their properties can be directly calculated. However, the situation is changing as the area is attracting more and more attention. Improvement of the HTS methods on one side and constant increase of computational power on another might reveal the option of simulating materials with large unit cells and covering more material properties.

Despite the fascinating progress of DL models, such approaches also have certain disadvantages, such as insufficient interpretability of models [215]. All large ML models are used as a kind of black box. Furthermore, the generalizability of these models remains a significant concern.

Also, one of the important disadvantages of all results achieved by data-driven approaches is that these results are purely theoretical and have not been presented in comparison with experimental data, and the difference can be significant. Currently, the experimental data are insufficient. Experimentation remains the bottleneck in the problem of material design.

An automated laboratory for searching, synthesizing and testing (measuring) materials would solve this problem of automatizing experimental material search and data acquisition. The first prototypes have already been demonstrated [216, 217]. Production and measurement of 2D materials on demand in a feedback loop with self-correcting ML algorithms will be a game-changing milestone.

Overall, progress in this area shows that the class of 2D materials and their derivatives is little studied, and there are many materials with potentially unique properties that have not yet been synthesized. Everything indicates that in the near future, we will have many discoveries in this area, some of which lie on the surface.

Acknowledgment

The article/review was prepared within the framework of the project 'Mirror Laboratories' HSE University, RF. This research / project is supported by the Ministry of Education, Singapore, under its Research Centre of Excellence award to the Institute for Functional Intelligent Materials (I-FIM, project No. EDUNC-33-18-279-V12). K.S.N. is grateful to the Royal Society (UK, grant number RSRP\R\190000) for support.

Data availability statement

No new data were created or analysed in this study.

Appendix A. Inverse problem in natural sciences

One of the earliest examples of an inverse problem is the determination of the shape of a hill from the travel time of a sliding particle on that hill [218], which was solved by Niels Henrik Abel in 1826 [219–222]. This work is generally accepted as the first formal mathematical solution to the inverse problem. However, unlike Abel's problem, which can be solved analytically, many inverse problems are difficult to solve analytically due to their complexity and ill-posed nature. In these cases, different numerical methods are used to approximate the solution by incorporating assumptions and inductive biases in the form of priors and regularizers to restrict the solution space [223–225].

The inverse problem in NDT, which involves determining the specimen parameters based on the response signal from an NDT probe [226–230], has studied the various techniques and applications of NDT.

In the medical field, inverse problem solutions have a wide range of applications, including medical imaging to construct images of internal tissue structures and diagnose diseases [231–236], radiation therapy [237–241], and cardiology as a part

of computational fluid dynamics to model fluid flow based on pressure, velocity, and other measurements [242–246].

In geology, inverse problems are used to infer the interior structure or properties of the Earth in terms of density and magnetism, or earthquake data analysis [247, 248] by analyzing data from various sources such as seismology, gravity, and magnetometry. This type of analysis can help scientists understand the composition and dynamics of the Earth's interior, which is important for understanding processes such as plate tectonics and volcanic activity. Additionally, inverse problems are used in astronomy to infer information about the properties of celestial objects and the Universe based on measurements of electromagnetic waves, such as light and radio waves [249]. These techniques can be used to study a wide range of astronomical phenomena, such as the structure of stars [250, 251], the distribution of matter in galaxies [252, 253], and the properties of the cosmic microwave background radiation [254].

ORCID iDs

Abdalaziz Al-Maeeni https://orcid.org/0000-0002-3299-7293
Mikhail Lazarev https://orcid.org/0000-0003-2252-625X
Nikita Kazeev https://orcid.org/0000-0002-5699-7634
Andrey Ustyuzhanin https://orcid.org/0000-0001-7865-2357

References

[1] Lionheart W R B and Newton C J P 2007 Analysis of the inverse problem for determining nematic liquid crystal director profiles from optical measurements using singular value decomposition *New J. Phys.* **9** 63–63
[2] Molesky S, Lin Z, Piggott A Y, Jin W, Vucković J and Rodriguez A W 2018 Inverse design in nanophotonics *Nat. Photon.* **12** 659–70
[3] Zunger A 2018 Inverse design in search of materials with target functionalities *Nat. Rev. Chem.* **2** 1–16
[4] Long T, Fortunato N M, Opahle I, Zhang Y, Samathrakis I, Shen C, Gutfleisch O and Zhang H 2021 Constrained crystals deep convolutional generative adversarial network for the inverse design of crystal structures *npj Comput. Mater.* **7** 1–7
[5] Ren Z *et al* 2022 An invertible crystallographic representation for general inverse design of inorganic crystals with targeted properties **5** 314–35 (https://doi.org/10.1016/j.matt.2021.11.032)
[6] Maine E and Seegopaul P 2016 Accelerating advanced-materials commercialization *Nat. Mater.* **15** 487–91
[7] Sanchez-Lengeling B and Aspuru-Guzik A 2018 Inverse molecular design using machine learning: Generative models for matter engineering *Science* **361** 360–5
[8] Parr R G 1980 *Density Functional Theory of Atoms and Molecules* (Oxford University Press) (https://doi.org/10.1093/oso/9780195092769.001.0001)
[9] Choudhary K *et al* 2022 Recent advances and applications of deep learning methods in materials science *npj Comput. Mater.* **8** 59
[10] Schleder G R, Padilha A C, Acosta C M, Costa M and Fazzio A 2019 From dft to machine learning: recent approaches to materials science–a review *J. Phys. Mater.* **2** 032001
[11] Burke K 2012 Perspective on density functional theory *J. Chem. Phys.* **136** 150901
[12] Pan J 2021 Scaling up system size in materials simulation *Nat. Comput. Sci.* **1** 95–95
[13] Nakata A *et al* 2020 Large scale and linear scaling dft with the conquest code *J. Chem. Phys.* **152** 164112
[14] Lu B, Xia Y Ren Y, Xie M, Zhou L, Vinai G, Morton S A, Wee A T, van der Wiel W G and Zhang W 2024 When machine learning meets 2d materials: a review *Adv. Sci.* **11** 2305277
[15] Tersoff J 1989 Modeling solid-state chemistry: interatomic potentials for multicomponent systems *Phys. Rev.* B **39** 5566
[16] Stuart S J, Tutein A B and Harrison J A 2000 A reactive potential for hydrocarbons with intermolecular interactions *J. Chem. Phys.* **112** 6472–86
[17] Srinivasan S G, Van Duin A C and Ganesh P 2015 Development of a reaxff potential for carbon condensed phases and its application to the thermal fragmentation of a large fullerene *J. Phys. Chem.* A **119** 571–80
[18] Lindsay L and Broido D 2010 Optimized tersoff and brenner empirical potential parameters for lattice dynamics and phonon thermal transport in carbon nanotubes and graphene *Phys. Rev.* B **81** 205441
[19] Mortazavi B, Silani M, Podryabinkin E V, Rabczuk T, Zhuang X and Shapeev A V 2021 First-principles multiscale modeling of mechanical properties in graphene/borophene heterostructures empowered by machine-learning interatomic potentials *Adv. Mater.* **33** 2102807
[20] Behler J and Parrinello M 2007 Generalized neural-network representation of high-dimensional potential-energy surfaces *Phys. Rev. Lett.* **98** 146401
[21] Mortazavi B, Zhuang X, Rabczuk T and Shapeev A V 2023 Atomistic modeling of the mechanical properties: the rise of machine learning interatomic potentials *Mater. Horiz.* **10** 1956–68
[22] Anstine D M and Isayev O 2023 Machine learning interatomic potentials and long-range physics *J. Phys. Chem.* A **127** 2417–31
[23] Wen T, Zhang L, Wang H, Weinan E and Srolovitz D J 2022 Deep potentials for materials science *Mater. Futures* **1** 022601
[24] Thompson A P *et al* 2022 LAMMPS—a flexible simulation tool for particle-based materials modeling at the atomic, meso and continuum scales *Comput. Phys. Commun.* **271** 108171
[25] Doerr S, Majewsk M, Pérez A Krämer A, Clementi C, Noe F, Giorgino T and Fabritiis G D 2020 Torchmd: a deep learning framework for molecular simulations (arXiv:2012.12106 [physics.chem-ph])
[26] Wang H, Zhang L, Han J and Weinan E 2018 Deepmd-kit: a deep learning package for many-body potential energy representation and molecular dynamics *Comput. Phys. Commun.* **228** 178–84
[27] Gubaev K, Podryabinkin E V, Hart G L and Shapeev A V 2019 Accelerating high-throughput searches for new alloys with active learning of interatomic potentials *Comput. Mater. Sci.* **156** 148–56
[28] Podryabinkin E V, Tikhonov E V, Shapeev A V and Oganov A R 2019 Accelerating crystal structure prediction by machine-learning interatomic potentials with active learning *Phys. Rev.* B **99** 064114
[29] Lu D, Wang H, Chen M, Lin L, Car R, Weinan E, Jia W and Zhang L 2021 86 PFLOPS deep potential molecular dynamics simulation of 100 million atoms with ab initio accuracy *Comput. Phys. Commun.* **259** 107624
[30] Mortazavi B, Novikov I S, Podryabinkin E V, Roche S, Rabczuk T, Shapeev A V and Zhuang X 2020 Exploring phononic properties of two-dimensional materials using

machine learning interatomic potentials *Appl. Mater. Today* **20** 100685
[31] Chen C and Ong S P 2022 A universal graph deep learning interatomic potential for the periodic table *Nat. Comput. Sci.* **2** 718–28
[32] Bartók A P, Payne M C, Kondor R and Csányi G 2010 Gaussian approximation potentials: The accuracy of quantum mechanics, without the electrons *Phys. Rev. Lett.* **104** 136403
[33] Novikov I S, Gubaev K, Podryabinkin E V and Shapeev A V 2020 The MLIP package: moment tensor potentials with mpi and active learning *Mach. Learn.: Sci. Technol.* **2** 025002
[34] Shapeev A V 2016 Moment tensor potentials: A class of systematically improvable interatomic potentials *Multiscale Model. Simul.* **14** 1153–73
[35] Thompson A P, Swiler L P, Trott C R, Foiles S M and Tucker G J 2015 Spectral neighbor analysis method for automated generation of quantum-accurate interatomic potentials *J. Comput. Phys.* **285** 316–30
[36] Schütt K T, Arbabzadah F, Chmiela S, Müller K R and Tkatchenko A 2017 Quantum-chemical insights from deep tensor neural networks *Nat. Commun.* **8** 13890
[37] Zaverkin V and Kaccstner J 2020 Gaussian moments as physically inspired molecular descriptors for accurate and scalable machine learning potentials *J. Chem. Theory Comput.* **16** 5410–21
[38] Fan Z, Zeng Z, Zhang C, Wang Y, Song K, Dong H, Chen Y and Ala-Nissila T 2021 Neuroevolution machine learning potentials: combining high accuracy and low cost in atomistic simulations and application to heat transport *Phys. Rev.* B **104** 104309
[39] Fan Q *et al* 2021 Biphenylene network: a nonbenzenoid carbon allotrope *Science* **372** 852–6
[40] Hou L, Cui X, Guan B, Wang S, Li R, Liu Y, Zhu D and Zheng J 2022 Synthesis of a monolayer fullerene network *Nature* **606** 507–10
[41] Seo T H, Lee W, Lee K S, Hwang J Y, Son D I, Ahn S, Cho H and Kim M J 2021 Dominant formation of h-bc2n in h-bxcynz films: Cvd synthesis and characterization *Carbon* **182** 791–8
[42] Marmolejo-Tejada J M and Mosquera M A 2022 Thermal properties of single-layer MoS_2–WS_2 alloys enabled by machine-learned interatomic potentials *Chem. Commun.* **58** 6902–5
[43] Li S, Liu Y, Chen D, Jiang Y, Nie Z and Pan F 2022 Encoding the atomic structure for machine learning in materials science *Wiley Interdiscip. Rev.-Comput. Mol. Sci.* **12** e1558
[44] Jones J E 1924 On the determination of molecular fields. I. From the variation of the viscosity of a gas with temperature *Proc. R. Soc.* A **106** 441–62
[45] Burden F R, Polley M J and Winkler D A 2009 Toward novel universal descriptors: charge fingerprints *J. Chem. Inform. Model.* **49** 710–5
[46] Dong J, Cao D-S, Miao H-Y, Liu S, Deng B-C, Yun Y-H, Wang N-N, Lu A-P, Zeng W-B and Chen A F 2015 Chemdes: an integrated web-based platform for molecular descriptor and fingerprint computation *J. Cheminform.* **7** 12
[47] Winter R, Montanari F, Noé F and Clevert D-A 2018 Learning continuous and data-driven molecular descriptors by translating equivalent chemical representations (available at: https://doi.org/10.26434/chemrxiv.6871628.v1)
[48] Wale N, Watson I A and Karypis G 2007 Comparison of descriptor spaces for chemical compound retrieval and classification *Knowl. Inform. Sys.* **14** 347–75
[49] Jiang Y, Yang Z, Guo J, Li H, Liu Y, Guo Y, long Li M and Pu X 2021 Coupling complementary strategy to flexible graph neural network for quick discovery of coformer in diverse co-crystal materials *Nat. Commun.* **12** 5950
[50] Singh Y, Sharma S K and Hazra P 2022 Mathematical analysis of one-dimensional lead sulphide crystal structure using molecular graph theory *Mol. Phys.* **120** 12
[51] Jiang Y, Guo J, Liu Y, Guo Y, Li M Y and Pu X 2021 A universal deep learning framework based on graph neural network for virtual co-crystal screening *ChemRxiv* (Cambridge university press) (https://doi.org/10.26434/chemrxiv.13514903.v1)
[52] Balasingham J, Zamaraev V and Kurlin V 2022 Compact graph representation of molecular crystals using point-wise distance distributions (arXiv:2212.11246)
[53] Shui Z, Karls D S, Wen M, Nikiforov I A, Tadmor E B and Karypis G 2022 Injecting domain knowledge from empirical interatomic potentials to neural networks for predicting material properties (arXiv:2210.08047)
[54] Rohskopf A, Seyf H R, Gordiz K, Tadano T and Henry A 2017 Empirical interatomic potentials optimized for phonon properties *npj Comput. Mater.* **3** 1–7
[55] Ito T, Akiyama T and Nakamura K 2016 Systematic approach to developing empirical interatomic potentials for III–N semiconductors *Jpn. J. Appl. Phys.* **55** 05FM02
[56] Warr W A 2011 Representation of chemical structures *Wiley Interdiscip. Rev.-Comput. Mol. Sci.* **1** 557–79
[57] Ziletti A, Kumar D, Scheffler M and Ghiringhelli L M 2018 Insightful classification of crystal structures using deep learning *Nat. Commun.* **9** 2775
[58] Tchagang A B and Valdés J J 2019 Prediction of the atomization energy of molecules using coulomb matrix and atomic composition in a bayesian regularized neural networks *Int. Conf. on Artificial Neural Networks* (Springer) pp 793–803
[59] Hansen K, Biegler F, Ramakrishnan R, Pronobis W, Von Lilienfeld O A, Mucccller K-R and Tkatchenko A 2015 Machine learning predictions of molecular properties: accurate many-body potentials and nonlocality in chemical space *J. Phys. Chem. Lett.* **6** 2326–31
[60] Dronskowski R and Bloechl P E 1993 Crystal orbital hamilton populations (COHP): energy-resolved visualization of chemical bonding in solids based on density-functional calculations *J. Phys. Chem.* **97** 8617–24
[61] Warshel A and Florián J 2004 The empirical valence bond (EVB) method (Wiley) (https://doi.org/10.1002/0470845015.cu0002)
[62] Pietrucci F and Andreoni W 2011 Graph theory meets ab initio molecular dynamics: atomic structures and transformations at the nanoscale *Phys. Rev. Lett.* **107** 085504
[63] Zhu L *et al* 2016 A fingerprint based metric for measuring similarities of crystalline structures *J. Chem. Phys.* **144** 034203
[64] Kajita S, Ohba N, Jinnouchi R and Asahi R 2017 A universal 3d voxel descriptor for solid-state material informatics with deep convolutional neural networks *Sci. Rep.* **7** 1–9
[65] Weiler M and Cesa G 2019 General E(2)-equivariant steerable CNNs *Advances in Neural Information Processing Systems* vol 32
[66] Xie T and Grossman J C 2018 Crystal graph convolutional neural networks for an accurate and interpretable prediction of material properties *Phys. Rev. Lett.* **120** 145301
[67] Weininger D, Weininger A and Weininger J L 1989 Smiles. 2. algorithm for generation of unique smiles notation *J. Chem. Inf. Comput. Sci.* **29** 97–101
[68] O'Boyle N M 2012 Towards a universal SMILES representation—a standard method to generate canonical SMILES based on the InChI *J. Cheminform.* **4** 22
[69] Krenn M *et al* 2022 Selfies and the future of molecular string representations *Patterns* **3** 100588
[70] Xiao H, Li R, Shi X, Chen Y, Zhu L, Chen X and Wang L 2023 An invertible, invariant crystal representation for inverse design of solid-state materials using generative deep learning *Nat. Commun.* **14** 7027

[71] Musil F, Grisafi A, Bartók A P, Ortner C, Csányi G and Ceriotti M 2021 Physics-inspired structural representations for molecules and materials *Chem. Rev.* **121** 9759–815
[72] Haastrup S *et al* 2018 The computational 2d materials database: high-throughput modeling and discovery of atomically thin crystals *2D Mater.* **5** 042002
[73] Gjerding M N *et al* 2021 Recent progress of the computational 2d materials database (C2DB) *2D Mater.* **8** 044002
[74] Huang P, Lukin R, Faleev M, Kazeev N, Al-Maeeni A R, Andreeva D V, Ustyuzhanin A, Tormasov A, Castro Neto A and Novoselov K S 2023 Unveiling the complex structure-property correlation of defects in 2d materials based on high throughput datasets *npj 2D Mater. Appl.* **7** 6
[75] Goodfellow I, Bengio Y and Courville A 2016 *Deep Learning* (MIT Press)
[76] Rombach R, Blattmann A, Lorenz D, Esser P and Ommer B 2022 High-resolution image synthesis with latent diffusion models (arXiv:2112.10752)
[77] Radford A, Kim J W, Xu T, Brockman G, McLeavey C and Sutskever I 2022 Robust speech recognition via large-scale weak supervision (arXiv:2212.04356)
[78] Brown T B *et al* 2020 Language models are few-shot learners (arXiv:2005.14165)
[79] Silver D *et al* 2016 Mastering the game of Go with deep neural networks and tree search *Nature* **529** 484–9
[80] Jumper J *et al* 2021 Highly accurate protein structure prediction with AlphaFold *Nature* **596** 583–9
[81] Ma X-Y, Lyu H-Y, Hao K-R, Zhao Y-M, Qian X, Yan Q-B and Su G 2021 Large family of two-dimensional ferroelectric metals discovered via machine learning *Sci. Bull.* **66** 233–42
[82] Willhelm D, Wilson N, Arroyave R, Qian X, Cagin T, Pachter R and Qian X 2022 Predicting van der waals heterostructures by a combined machine learning and density functional theory approach *ACS Appl. Mater. Interfaces* **14** 25907–19
[83] Tang J-l, Cai Q-R and Liu Y-I 2010 Prediction of material mechanical properties with support vector machine *2010 Int. Conf. on Machine Vision and Human-Machine Interface* (IEEE) pp 592–5
[84] Balachandran P V, Theiler J, Rondinelli J M and Lookman T 2015 Materials prediction via classification learning *Sci. Rep.* **5** 13285
[85] Schleder G R, Acosta C M and Fazzio A 2019 Exploring two-dimensional materials thermodynamic stability via machine learning *ACS Appl. Mater. Interfaces* **12** 20149–57
[86] Tawfik S A, Isayev O, Stampfl C, Shapter J, Winkler D A and Ford M J 2019 Efficient prediction of structural and electronic properties of hybrid 2d materials using complementary dft and machine learning approaches *Adv. Theory Simul.* **2** 1800128
[87] Gu J *et al* 2018 Recent advances in convolutional neural networks *Pattern Recognit.* **77** 354–77
[88] Li X *et al* 2021 Ordered clustering of single atomic te vacancies in atomically thin ptte2 promotes hydrogen evolution catalysis *Nat. Commun.* **12** 2351
[89] Choudhary K, DeCost B and Tavazza F 2018 Machine learning with force-field-inspired descriptors for materials: Fast screening and mapping energy landscape *Phys. Rev. Mater.* **2** 083801
[90] Lam Pham T, Kino H, Terakura K, Miyake T, Tsuda K, Takigawa I and Chi Dam H 2017 Machine learning reveals orbital interaction in materials *Sci. Technol. Adv. Mater.* **18** 756–65
[91] Ong S P, Richards W D, Jain A, Hautier G, Kocher M, Cholia S, Gunter D, Chevrier V L, Persson K A and Ceder G 2013 Python Materials Genomics (pymatgen): a robust, open-source python library for materials analysis *Comput. Mater. Sci.* **68** 314–9
[92] Krivovichev S V 2013 Structural complexity of minerals: information storage and processing in the mineral world *Mineral. Mag.* **77** 275–326
[93] Schütt K, Kindermans P-J, Sauceda Felix H E, Chmiela S, Tkatchenko A and Müller K-R 2017 Schnet: a continuous-filter convolutional neural network for modeling quantum interactions *Advances in Neural Information Processing Systems* vol 30
[94] Ruddigkeit L, Van Deursen R, Blum L C and Reymond J-L 2012 Enumeration of 166 billion organic small molecules in the chemical Universe database gdb-17 *J. Chem. Inform. Model.* **52** 2864–75
[95] Ramakrishnan R, Dral P O, Rupp M and von Lilienfeld O A 2014 Quantum chemistry structures and properties of 134 kilo molecules *Sci. Data* **1** 140022
[96] Chmiela S, Tkatchenko A, Sauceda H E, Poltavsky I, Schütt K T and Müller K-R 2017 Machine learning of accurate energy-conserving molecular force fields *Sci. Adv.* **3** e1603015
[97] Battaglia P W *et al* 2018 Relational inductive biases, deep learning, and graph networks (arXiv:1806.01261)
[98] Kipf T N and Welling M 2017 Semi-supervised classification with graph convolutional networks (arXiv:1609.02907)
[99] Zhou J, Cui G, Hu S, Zhang Z, Yang C, Liu Z, Wang L, Li C and Sun M 2020 Graph neural networks: a review of methods and applications *AI Open* **1** 57–81
[100] Li C-N, Liang H-P, Zhang X, Lin Z and Wei S-H 2023 Graph deep learning accelerated efficient crystal structure search and feature extraction *npj Comput. Mater.* **9** 176
[101] Chen C, Ye W, Zuo Y, Zheng C and Ong S P 2019 Graph networks as a universal machine learning framework for molecules and crystals *Chem. Mater.* **31** 3564–72
[102] Gasteiger J, Groß J and Günnemann S 2022 Directional message passing for molecular graphs (arXiv:2003.03123)
[103] Gasteiger J, Giri S, Margraf J T and Günnemann S 2022 Fast and uncertainty-aware directional message passing for non-equilibrium molecules (arXiv2011.14115)
[104] Louis S-Y, Zhao Y, Nasiri A, Wang X, Song Y, Liu F and Hu J 2020 Graph convolutional neural networks with global attention for improved materials property prediction *Phys. Chem. Chem. Phys.* **22** 18141–8
[105] Gasteiger J, Becker F and Günnemann S 2021 Gemnet: universal directional graph neural networks for molecules *Advances in Neural Information Processing Systems* vol 34 pp 6790–802
[106] Brock A, De S and Smith S L 2021 Characterizing signal propagation to close the performance gap in unnormalized ResNets (arXiv:2101.08692)
[107] Pollice R *et al* 2021 Data-driven strategies for accelerated materials design *Acc. Chem. Res.* **54** 849–60
[108] Song D, Chen X, Lin Z Tang Z , Ma W, Zhang Q, Li Y and Zhang X 2021 Usability identification framework and high-throughput screening of two-dimensional materials in lithium ion batteries *ACS Nano* **15** 16469–77
[109] Li X, Zhang Z, Yao Y and Zhang H 2018 High throughput screening for two-dimensional topological insulators *2D Mater.* **5** 045023
[110] Sarikurt S, Kocabaş T and Sevik C 2020 High-throughput computational screening of 2d materials for thermoelectrics *J. Mater. Chem.* A **8** 19674–83
[111] Zhang X, Chen A and Zhou Z 2019 High-throughput computational screening of layered and two-dimensional materials *WIREs Comput. Mol. Sci.* **9** e1385
[112] Zhang X, Zhang Z, Yao S, Chen A, Zhao X and Zhou Z 2018 An effective method to screen sodium-based layered materials for sodium ion batteries *npj Comput. Mater.* **4** 13
[113] Mounet N *et al* 2018 Two-dimensional materials from high-throughput computational exfoliation of experimentally known compounds *Nat. Nanotechnol.* **13** 246–52
[114] Olsen T 2016 Designing in-plane heterostructures of quantum spin Hall insulators from first principles: 1T–MoS_2 with adsorbates *Phys. Rev.* B **94** 235106

[115] Padilha J E, Pontes R B, Schmidt T M, Miwa R H and Fazzio A 2016 A new class of large band gap quantum spin hall insulators: 2D fluorinated group-IV binary compounds *Sci. Rep.* **6** 26123
[116] Xu Y, Yan B, Zhang H-J, Wang J, Xu G, Tang P, Duan W and Zhang S-C 2013 Large-Gap Quantum Spin Hall Insulators in Tin Films *Phys. Rev. Lett.* **111** 136804
[117] Yu W, Niu C-Y, Zhu Z, Cai X, Zhang L, Bai S, Zhao R and Jia Y 2017 Strain induced quantum spin Hall insulator in monolayer β-BiSb from first-principles study *RSC Adv.* **7** 27816–22
[118] Zhang R-W, Zhang C-W, Ji W-X, Yan S-S and Yao Y-G 2017 Correction: First-principles prediction on bismuthylene monolayer as a promising quantum spin Hall insulator *Nanoscale* **9** 11814–5
[119] Novoselov K S, Geim A K, Morozov S V, Jiang D, Zhang Y, Dubonos S V, Grigorieva I V and Firsov A A 2004 Electric field effect in atomically thin carbon films *Science* **306** 666–9
[120] Nicolosi V, Chhowalla M, Kanatzidis M G, Strano M S and Coleman J N 2013 Liquid exfoliation of layered materials *Science* **340** 1226419
[121] Coleman J N *et al* 2011 Two-dimensional nanosheets produced by liquid exfoliation of layered materials *Science* **331** 568–71
[122] Li L, Yu Y, Ye G J, Ge Q, Ou X, Wu H, Feng D, Chen X H and Zhang Y 2014 Black phosphorus field-effect transistors *Nat. Nanotechnol.* **9** 372–7
[123] Naguib M, Mochalin V N, Barsoum M W and Gogotsi Y 2014 25th anniversary article: MXenes: a new family of two-dimensional materials *Adv. Mater.* **26** 992–1005
[124] Noh J, Gu G H, Kim S and Jung Y 2020 Uncertainty-quantified hybrid machine learning/density functional theory high throughput screening method for crystals *J. Chem. Inform. Model.* **60** 1996–2003
[125] Park C W and Wolverton C 2020 Developing an improved crystal graph convolutional neural network framework for accelerated materials discovery *Phys. Rev. Mater.* **4** 063801
[126] Gal Y and Ghahramani Z 2016 Dropout as a Bayesian approximation: representing model uncertainty in deep learning (arXiv:1506.02142)
[127] Merchant A, Batzner S, Schoenholz S S, Aykol M, Cheon G and Cubuk E D 2023 Scaling deep learning for materials discovery *Nature* **624** 1–6
[128] Szymanski N J *et al* 2023 An autonomous laboratory for the accelerated synthesis of novel materials *Nature* **624** 1–6
[129] Katoch S, Chauhan S S and Kumar V 2021 A review on genetic algorithm: Past, present and future *Multimedia Tools Appl.* **80** 8091–126
[130] Darwin C 1859 *On the Origin of Species by Means of Natural Selection* (Murray)
[131] Metaheuristics classification (available at: https://commons.wikimedia.org/wiki/File:Metaheuristics_classification.svg) (Accessed 11 May 2023)
[132] Johnson J M and Rahmat-Samii Y 1994 Genetic algorithm optimization and its application to antenna design *Proc. IEEE Antennas and Propagation Society Int. Symp. and URSI National Radio Science Meeting* vol 1 (IEEE) pp 326–9
[133] Sloss A N and Gustafson S 2020 2019 evolutionary algorithms review *Genetic Programming Theory and Practice XVII* pp 307–44
[134] Håkansson A and Sanchez-Dehesa J 2005 Inverse designed photonic crystal de-multiplex waveguide coupler *Opt. Express* **13** 5440–9
[135] Joannopoulos J 2008 *Photonic Crystals: Molding the Flow of Light - Second Edition* (Princeton University Press) (https://doi.org/10.1515/9781400828241) (available at: https://press.princeton.edu/books/hardcover/9780691124568/photonic-crystals)
[136] John S 1987 Strong localization of photons in certain disordered dielectric superlattices *Phys. Rev. Lett.* **58** 2486–9
[137] Gan L and Li Z 2015 Photonic crystal cavities and integrated optical devices *Sci. China Phys. Mech. Astron.* **58** 114203
[138] Rifqi Md Zain A and De La Rue R M 2019 Modelling of photonic crystal (PhC) cavities: theory and applications *Photonic Crystals—A Glimpse of the Current Research Trends* (IntechOpen)
[139] Zhao Y, Shang L, Cheng Y and Gu Z 2014 Spherical colloidal photonic crystals *Acc. Chem. Res.* **47** 3632–42
[140] Spühler M M, Erni D and Fröhlich J 1998 An evolutionary optimization procedure applied to the synthesis of integrated spot-size converters *Opt. Quantum Electron.* **30** 305–21
[141] Shen L, Ye Z and He S 2003 Design of two-dimensional photonic crystals with large absolute band gaps using a genetic algorithm *Phys. Rev.* B **68** 035109
[142] Geremia J, Williams J and Mabuchi H 2002 Inverse-problem approach to designing photonic crystals for cavity qed experiments *Phys. Rev.* E **66** 066606
[143] Håkansson A, Sanchis P, Sánchez-Dehesa J and Martí J 2005 High-efficiency defect-based photonic-crystal tapers designed by a genetic algorithm *J. Lightwave Technol.* **23** 3881 (available at: https://opg.optica.org/jlt/abstract.cfm?URI=jlt-23-11-3881)
[144] Håkansson A and Sánchez-Dehesa J 2005 Inverse designed photonic crystal de-multiplex waveguide coupler *Opt. Express* **13** 5440–9
[145] Kildishev A V, Chettiar U K, Liu Z, Shalaev V M, Kwon D-H, Bayraktar Z and Werner D H 2007 Stochastic optimization of low-loss optical negative-index metamaterial *J. Opt. Soc. Am.* B **24** A34–A39
[146] Hassan H and Tallman T N 2021 A comparison of metaheuristic algorithms for solving the piezoresistive inverse problem in self-sensing materials *IEEE Sens. J.* **21** 659–66
[147] Chung D 2016 Self-sensing structural composites in aerospace engineering *Advanced Composite Materials for Aerospace Engineering* (Elsevier) pp 295–331
[148] Rana S, Subramani P, Fangueiro R and Gomes Correia A 2016 A review on smart self-sensing composite materials for civil engineering applications *AIMS Mater. Sci.* **3** 357–79
[149] Laflamme S and Ubertini F 2020 Back-to-basics: self-sensing materials for nondestructive evaluation *Mater. Eval* **78** 526–36 (available at: https://faculty.sites.iastate.edu/laflamme/files/inline-files/Laflamme_J72_2019.pdf)
[150] Swait T J, Rauf A, Grainger R, Bailey P B S, Lafferty A D, Fleet E J, Hand R J and Hayes S A 2012-06 Smart composite materials for self-sensing and self-healing *Plast. Rubber Compos.* **41** 215–24
[151] Thostenson E T and Chou T-W 2007 Multifunctional composites with self-sensing capabilities: carbon nanotube-based networks *Behavior and Mechanics of Multifunctional and Composite Materials 2007* ed M J Dapino (SPIE)(https://doi.org/10.1117/12.715434)
[152] Tian Z, Li Y, Zheng J and Wang S 2019-11 A state-of-the-art on self-sensing concrete: Materials, fabrication and properties *Composites* B **177** 107437
[153] Vlachakis C, Perry M and Biondi L 2020 Self-sensing alkali-activated materials: a review *Minerals* **10** 885
[154] Ingber L 2000 Adaptive simulated annealing (ASA): lessons learned (arXiv:cs/0001018)
[155] Metropolis N, Rosenbluth A W, Rosenbluth M N, Teller A H and Teller E 1953-06 Equation of state calculations by fast computing machines *J. Chem. Phys.* **21** 1087–92
[156] Kennedy J and Eberhart R 1995 Particle swarm optimization *Proc. ICNN'95—Int. Conf. on Neural Networks* vol 4 pp 1942–8
[157] Pedersen M E H 2010 Good parameters for particle swarm optimization *Technical Report HL1001* (Hvass Lab)
[158] Mezura-Montes E and Coello Coello C A 2011 Constraint-handling in nature-inspired numerical

optimization: past, present and future *Swarm Evolut. Comput.* **1** 173–94
[159] Raghavan S, Imbrie P K and Crossley W A 2008 Spectral analysis of R-lines and vibronic sidebands in the emission spectrum of Ruby using genetic algorithms *Appl. Spectrosc.* **62** 759–65
[160] Hassan H and Tallman T N 2020 Failure prediction in self-sensing nanocomposites via genetic algorithm-enabled piezoresistive inversion *Struct. Health Monit.* **19** 765–80
[161] Zhao Y, Zeng S and Ni J 2016 Superconductivity in two-dimensional boron allotropes *Phys. Rev.* B **93** 014502
[162] Oganov A R and Glass C W 2006 Crystal structure prediction using ab initio evolutionary techniques: Principles and applications *J. Chem. Phys.* **124** 244704
[163] Zhu Q, Li L, Oganov A R and Allen P B 2013 Evolutionary method for predicting surface reconstructions with variable stoichiometry *Phys. Rev.* B **87** 195317
[164] Glass C W, Oganov A R and Hansen N 2006-12 USPEX—evolutionary crystal structure prediction *Comput. Phys. Commun.* **175** 713–20
[165] Zhang W, Oganov A R, Goncharov A F, Zhu Q, Boulfelfel S E, Lyakhov A O, Stavrou E, Somayazulu M, Prakapenka V B and Konôpková Z 2013 Unexpected stable stoichiometries of sodium chlorides *Science* **342** 1502–5
[166] Shi G, Chen L, Yang Y, Li D, Qian Z, Liang S, Yan L, Li L H, Wu M and Fang H 2018 Two-dimensional Na–Cl crystals of unconventional stoichiometries on graphene surface from dilute solution at ambient conditions *Nat. Chem.* **10** 776–9
[167] Faraji S, Wang B, Valencia H O and Frapper G 2021 Computational discovery of two-dimensional copper chalcogenides CuX (X = S, Se, Te) *Phys. Rev. Mater.* **5** 124007
[168] Popov Z I, Tikhomirova K A, Demin V A, Chowdhury S, Oganov A R, Kvashnin A G and Kvashnin D G 2021 Novel two-dimensional boron oxynitride predicted using the uspex evolutionary algorithm *Phys. Chem. Chem. Phys.* **23** 26178–84
[169] Bahmann S and Kortus J 2013 EVO—evolutionary algorithm for crystal structure prediction *Comput. Phys. Commun.* **184** 1618–25
[170] Woodley S and Catlow R 2009 Structure prediction of titania phases: implementation of Darwinian versus Lamarckian concepts in an evolutionary algorithm *Comput. Mater. Sci.* **45** 84–95
[171] Tong W-Y, Gong S-J, Wan X and Duan C-G 2016 Concepts of ferrovalley material and anomalous valley Hall effect *Nat. Commun.* **7** 13612
[172] Liu Y, Zeng C, Zhong J, Ding J, Wang Z M and Liu Z 2020 Spintronics in Two-Dimensional Materials *Nano-Micro Lett.* **12** 93
[173] Huang B *et al* 2017 Layer-dependent ferromagnetism in a van der Waals crystal down to the monolayer limit *Nature* **546** 270–3
[174] Gong C *et al* 2017 Discovery of intrinsic ferromagnetism in 2D van der Waals crystals *Nature* **546** 265–9
[175] Bonilla M, Kolekar S, Ma Y, Diaz H C, Kalappattil V, Das R, Eggers T, Gutierrez H R, Phan M-H and Batzill M 2018 Strong room-temperature ferromagnetism in VSe2 monolayers on van der Waals substrates *Nat. Nanotechnol.* **13** 289–93
[176] Awan S U, Zainab S, Khan M D, Rizwan S and Iqbal M Z 2020 2-Dimensional magnetic materials for spintronics technology *Nanoscience* (Royal Society of Chemistry) pp 91–119
[177] Ahn E C 2020 2D materials for spintronic devices *npj 2D Mater. Appl.* **4** 17
[178] Chen S, Yue Y and Liu J 2022 Constrained optimization of transition metal dichalcogenide-based Bloch surface wave sensor using improved genetic algorithm *Appl. Phys.* A **128** 945
[179] Mishra A, Hong S, Rajak P, Sheng C, Nomura K-i, Kalia R K, Nakano A and Vashishta P 2018 Multiobjective genetic training and uncertainty quantification of reactive force fields *npj Comput. Mater.* **4** 1–7
[180] Duin P U, Adri C T, Dasgupta S, Lorant F and Goddard W A 2001 ReaxFF: A Reactive Force Field for Hydrocarbons *J. Phys. Chem.* A **105** 9396–409
[181] Patra T K, Meenakshisundaram V, Hung J-H and Simmons D S 2017 Neural-network-biased genetic algorithms for materials design: evolutionary algorithms that learn *ACS Combin. Sci.* **19** 96–107
[182] Patra T K, Zhang F, Schulman D S, Chan H, Cherukara M J, Terrones M, Das S, Narayanan B and Sankaranarayanan S K 2018 Defect dynamics in 2-d MoS_2 probed by using machine learning, atomistic simulations and high-resolution microscopy *ACS Nano* **12** 8006–16
[183] Dong R, Song Y, Siriwardane E M D and Hu J 2023 Discovery of 2D materials using transformer network based generative design (arXiv:2301.05824)
[184] Vaswani A, Shazeer N, Parmar N, Uszkoreit J, Jones L, Gomez A N, Kaiser Ł and Polosukhin I 2017 Attention is all you need *Advances in Neural Information Processing Systems* vol 30 (available at: https://proceedings.neurips.cc/paper_files/paper/2017/hash/3f5ee243547dee91fbd053c1c4a845aa-Abstract.html)
[185] Wei L, Fu N, Siriwardane E M, Yang W, Omee S S, Dong R, Xin R and Hu J 2022 Tcsp: a template-based crystal structure prediction algorithm for materials discovery *Inorg. Chem.* **61** 8431–9
[186] Kusaba M, Liu C and Yoshida R 2022 Crystal structure prediction with machine learning-based element substitution *Comput. Mater. Sci.* **211** 111496
[187] Zuo Y, Qin M, Chen C, Ye W, Li X, Luo J and Ong S P 2021 Accelerating materials discovery with bayesian optimization and graph deep learning *Mater. Today* **51** 126–35
[188] Kingma D P and Welling M 2013 Auto-encoding variational bayes (arXiv:1312.6114)
[189] Noh J, Kim J, Stein H S, Sanchez-Lengeling B, Gregoire J M, Aspuru-Guzik A and Jung Y 2019 Inverse design of solid-state materials via a continuous representation *Matter* **1** 1370–84
[190] Xie T, Fu X, Ganea O-E, Barzilay R and Jaakkola T 2021 Crystal diffusion variational autoencoder for periodic material generation (arXiv:2110.06197)
[191] Zeni C *et al* 2023 Mattergen: a generative model for inorganic materials design (arXiv:2312.03687)
[192] Agarwal A, Goverapet Srinivasan S and Rai B 2021 Data-driven discovery of 2D materials for solar water splitting *Front. Mater.* **8** 165384
[193] Jain A *et al* 2013 Commentary: the materials project: a materials genome approach to accelerating materials innovation *APL Mater.* **1** 011002
[194] Goodfellow I, Pouget-Abadie J, Mirza M, Xu B, Warde-Farley D, Ozair S, Courville A and Bengio Y 2020 Generative adversarial networks *Commun. ACM* **63** 139–44
[195] Yeung C, Tsai R, Pham B, King B, Kawagoe Y, Ho D, Liang J, Knight M W and Raman A P 2021 Global inverse design across multiple photonic structure classes using generative deep learning *Adv. Opt. Mater.* **9** 2100548
[196] Kim S, Noh J, Gu G H, Aspuru-Guzik A and Jung Y 2020 Generative adversarial networks for crystal structure prediction *ACS Cent. Sci.* **6** 1412–20
[197] Arjovsky M, Chintala S and Bottou L 2017 Wasserstein generative adversarial networks *Int. Conf. on Machine Learning* (PMLR) pp 214–23
[198] Long T, Zhang Y, Fortunato N M, Shen C, Dai M and Zhang H 2022 Inverse design of crystal structures for multicomponent systems *Acta Mater.* **231** 117898
[199] Song Y, Siriwardane E M D, Zhao Y and Hu J 2021 Computational discovery of new 2D materials using deep learning generative models *ACS Appl. Mater. Interfaces* **13** 53303–13

[200] Antunes L M, Butler K T and Grau-Crespo R 2023 Crystal structure generation with autoregressive large language modeling (arXiv:2307.04340)
[201] Flam-Shepherd D and Aspuru-Guzik A 2023 Language models can generate molecules, materials, and protein binding sites directly in three dimensions as XYZ, CIF, and PDB files (arXiv:2305.05708)
[202] Chen I-J, Aapro M, Kipnis A, Ilin A, Liljeroth P and Foster A S 2022 Precise atom manipulation through deep reinforcement learning *Nat. Commun.* **13** 7499
[203] Mousavi S S, Schukat M and Howley E 2018 Deep reinforcement learning: an overview *Proc. SAI Intelligent Systems Conf. (IntelliSys) 2016* vol 2 (Springer) pp 426–40 (available at: https://link.springer.com/chapter/10.1007/978-3-319-56991-8_32)
[204] Banik S, Loeffler T D, Batra R, Singh H, Cherukara M J and Sankaranarayanan S K 2021 Learning with delayed rewards—a case study on inverse defect design in 2d materials *ACS Appl. Mater. Interfaces* **13** 36455–64
[205] Rubin D B 1984 Bayesianly Justifiable and Relevant Frequency Calculations for the Applied Statistician *Ann. Stat.* **12** 1151–72
[206] Alsing J, Wandelt B and Feeney S 2018 Massive optimal data compression and density estimation for scalable, likelihood-free inference in cosmology *Mon. Not. R. Astron. Soc.* **477** 2874–85
[207] Charnock T, Lavaux G and Wandelt B D 2018 Automatic physical inference with information maximizing neural networks *Phys. Rev.* D **97** 083004
[208] Brehmer J, Louppe G, Pavez J and Cranmer K 2020 Mining gold from implicit models to improve likelihood-free inference *Proc. Natl Acad. Sci.* **117** 5242–9
[209] Cranmer K, Pavez J and Louppe G 2015 Approximating likelihood ratios with calibrated discriminative classifiers (arXiv:1506.02169)
[210] Stoye M, Brehmer J, Louppe G, Pavez J and Cranmer K 2018 Likelihood-free inference with an improved cross-entropy estimator (arXiv:1808.00973)
[211] Mohamed S and Lakshminarayanan B 2016 Learning in implicit generative models (arXiv:1610.03483)
[212] Louppe G, Hermans J and Cranmer K 2019 Adversarial variational optimization of non-differentiable simulators *22nd Int. Conf. on Artificial Intelligence and Statistics* (PMLR) pp 1438–47 (available at: https://proceedings.mlr.press/v89/louppe19a.html)
[213] Le T A, Baydin A G and Wood F 2017 Inference compilation and universal probabilistic programming *Artificial Intelligence and Statistics* (PMLR) pp 1338–48 (available at: https://proceedings.mlr.press/v54/le17a.html)
[214] Cranmer K, Brehmer J and Louppe G 2020 The frontier of simulation-based inference *Proc. Natl Acad. Sci.* **117** 30055–62
[215] Gilpin L H, Bau D, Yuan B Z, Bajwa A, Specter M and Kagal L 2018 Explaining explanations: An overview of interpretability of machine learning *2018 IEEE 5th Int. Conf. on Data Science and Advanced Analytics (DSAA)* (IEEE) pp 80–89
[216] Burger B *et al* 2020 A mobile robotic chemist *Nature* **583** 237–41
[217] Coley C W *et al* 2019 A robotic platform for flow synthesis of organic compounds informed by ai planning *Science* **365** eaax1566
[218] Frobenius Herrn *Journal Für Die Reine Und Angewandte Mathematik* (de Gruyter)(https://doi.org/10.1515/crelle-1878-18788403)
[219] Ab Azar N, Shahmansoorian A and Davoudi M 2020 From inverse optimal control to inverse reinforcement learning: a historical review *Annu. Rev. Control* **50** 119–38
[220] Keller J B 1976 Inverse problems *Am. Math. Mon.* **83** 107–18
[221] Yaman F, Yakhno V G and Potthast R 2013 A survey on inverse problems for applied sciences *Math. Probl. Eng.* **2013** e976837
[222] Groetsch C W 2007 Integral equations of the first kind, inverse problems and regularization: a crash course *J. Phys.: Conf. Ser.* **73** 012001
[223] Jin B and Zou J 2010 Hierarchical bayesian inference for ill-posed problems via variational method *J. Comput. Phys.* **229** 7317–43
[224] De Campos Velho H F, Ramos F M, Chalhoub E S, Stephany S, Carvalho J C and De Sousa F L 2007 Inverse problems in space science and technology *Inverse Problems Sci. Eng.* **15** 359–72
[225] Haber E, Horesh L and Tenorio L 2008 Numerical methods for experimental design of large-scale linear ill-posed inverse problems *Inverse Problems* **24** 055012
[226] Udpa L and Lord W 1986 A discussion of the inverse problem in electromagnetic NDT (https://doi.org/10.1007/978-1-4615-7763-8_38)
[227] Bilicz S, Lambert M, Gyimothy S and Pavo J 2012-02 Solution of inverse problems in nondestructive testing by a Kriging-based surrogate model *IEEE Trans. Magn.* **48** 495–8
[228] Blitz J 1983-12 Nondestructive testing using electromagnetic instrumentation *J. Phys. E: Sci. Instrum.* **16** 1135–41
[229] Langenberg K J, Brandfaß M, Klaholz S, Marklein R, Mayer K, Pitsch A and Schneider R 1997 Applied inversion in nondestructive testing *Inverse Problems in Medical Imaging and Nondestructive Testing* (Springer) pp 93–119 (available at: https://link.springer.com/chapter/10.1007/978-3-7091-6521-8_8
[230] Collins R 1995 *Nondestructive Testing of Materials* vol 8 (IOS Press) (available at: www.iospress.com/catalog/books/nondestructive-testing-of-materials)
[231] Aghajani A, Haghpanahi M and Nikazad T 2013 The ultrasound elastography inverse problem and the effective criteria *Proc. Inst. Mech. Eng.* H **227** 1203–12
[232] Burger M, Dirks H and Müller J 2013 Inverse problems in imaging *Large Scale Inverse Problems* (DE GRUYTER) pp 135–80
[233] Monard F 2012 (Columbia University) (available at: https://people.ucsc.edu/~fmonard/FrancoisMonardThesis.pdf)
[234] Pursiainen S 2008 Computational methods in electromagnetic biomedical inverse problems (Helsinki University of Technology) (available at: https://aaltodoc.aalto.fi/items/9c496c57-f736-401b-8c79-497c842b406b)
[235] Senouf O, Vedula S, Weiss T, Bronstein A, Michailovich O and Zibulevsky M 2019 Self-supervised learning of inverse problem solvers in medical imaging *Domain Adaptation and Representation Transfer and Medical Image Learning With Less Labels and Imperfect Data* (Springer International Publishing) pp 111–9 (available at: https://link.springer.com/book/10.1007/978-3-030-33391-1)
[236] Song Y, Shen L, Xing L and Ermon S 2022 Solving inverse problems in medical imaging with score-based generative models (arXiv:2111.08005)
[237] Alfonso J C L, Buttazzo G, García-Archilla B, Herrero M A and Núñez L 2012-05 A class of optimization problems in radiotherapy dosimetry planning *Discrete Contin. Dyn. Syst.* B **17** 1651–72
[238] Bertuzzi A, Bruni C, Papa F and Sinisgalli C 2012 Optimal solution for a cancer radiotherapy problem *J. Math. Biol.* **66** 311–49
[239] Buman C, Abut H, Al-Ghazi M and Yakoob R 2000 Applications of signal processing to conformal radiation therapy dose optimization *2000 IEEE Int. Conf. on Acoustics, Speech and Signal Processing. Proc. (Cat. No. 00CH37100)* (IEEE) (https://doi.org/10.1109/ICASSP.2000.860171)
[240] Hindi H 2013-06 A tutorial on optimization methods for cancer radiation treatment planning *2013 American Control Conf.* (IEEE)
[241] Jalalimanesh A, Haghighi H S, Ahmadi A, Hejazian H and Soltani M 2017 Multi-objective optimization of

radiotherapy: Distributed Q-learning and agent-based simulation *J. Exp. Theor. Artif. Intell.* **29** 1071–86
[242] Cotter S L, Dashti M, Robinson J C and Stuart A M 2009 Bayesian inverse problems for functions and applications to fluid mechanics *Inverse Problems* **25** 115008
[243] Fernández-Cara E, Horsin T and Kasumba H 2013 Some inverse and control problems for fluids *Ann. Math. Blaise Pascal* **20** 101–38
[244] Fourestey G and Moubachir M 2005-02 Solving inverse problems involving the Navier–Stokes equations discretized by a Lagrange–Galerkin method *Comput. Methods Appl. Mech. Eng.* **194** 877–906
[245] Gregson J 2015 Applications of inverse problems in fluids and imaging (University of British Columbia)(https://doi.org/10.14288/1.0166394)
[246] Imanuvilov O Y and Yamamoto M 2020 Inverse problems for a compressible fluid system *Springer Proc. in Mathematics & Statistics* (Springer) pp 101–48
[247] Barhen J *et al* 2000 Optimization and geophysical inverse problems (available at: http://dx.doi.org/10.2172/939130)
[248] Kim Y and Nakata N 2018-12 Geophysical inversion versus machine learning in inverse problems *Lead. Edge* **37** 894–901
[249] Brown J C 1995 Inverse problems in astrophysical spectrometry *Inverse Problems* **11** 783–94
[250] Bellinger E P 2018 Inverse problems in asteroseismology (arXiv:1808.06649)
[251] kun Tsui L, Leung P T and Wu J 2006 Determination of the internal structure of neutron stars from gravitational wave spectra *Phys. Rev.* D **74** 124025
[252] Daza G F-T and López-Corredoira M 2020Relationship between rotation curves and matter distribution in spiral galaxy discs (arXiv:2003.04951)
[253] Lanusse F, Leonard A and Starck J-L 2013 Imaging dark matter using sparsity *Optics Photonics—Optical Engineering + Applications* (https://doi.org/10.1117/12.2023811)
[254] Lassas M, Oksanen L, Stefanov P and Uhlmann G 2018 On the inverse problem of finding cosmic strings and other topological defects *Commun. Math. Phys.* **357** 569–95